Formation and locking of the "slinky mode" in reversed-field pinches

Richard Fitzpatrick

Articles you may be interested in

Resistive wall modes in the EXTRAP T2R reversed-field pinch
Phys. Plasmas **10**, 3823 (2003); 10.1063/1.1604775

Evolution process of the mode wall-locking and phase-locking in a reversed-field pinch plasma
Phys. Plasmas **8**, 1625 (2001); 10.1063/1.1364674

Locked modes in two reversed-field pinch devices of different size and shell system
Phys. Plasmas **7**, 4184 (2000); 10.1063/1.1290281

Mode-locking phenomena in the TPE-RX reversed-field pinch plasma
Phys. Plasmas **6**, 3824 (1999); 10.1063/1.873647

Locking of multiple resonant mode structures in the reversed-field pinch
Phys. Plasmas **5**, 2942 (1998); 10.1063/1.873017

Formation and locking of the ''slinky mode'' in reversed-field pinches

Richard Fitzpatrick

*Institute for Fusion Studies, Department of Physics, University of Texas at Austin,
Austin, Texas 78712-1060*

The formation and breakup of the ''slinky mode'' in a Reversed-Field Pinch (RFP) is investigated analytically. The slinky mode is a toroidally localized, coherent interference pattern in the magnetic field, which corotates with the plasma at the reversal surface. This mode forms, via a series of bifurcations, as a result of the nonlinear coupling of multiple $m=1$ core tearing modes. The slinky mode breaks up via a second series of bifurcations. However, the typical mode amplitude below which slinky breakup is triggered is much smaller than that above which slinky formation occurs. Analytic expressions for the slinky formation and breakup thresholds are obtained in all regimes of physical interest. The locking of the slinky mode to a static error field is also investigated analytically. Either the error field arrests the rotation of the plasma at the reversal surface before the formation of the slinky mode, so that the mode subsequently forms as a nonrotating mode, or the slinky mode forms as a rotating mode and subsequently locks to the error field. Analytic expressions for the locking and unlocking thresholds are obtained in all regimes of physical interest. © *1999 American Institute of Physics.* [S1070-664X(99)02604-X]

I. INTRODUCTION

A reversed-field pinch (or RFP) is a magnetic fusion device that is similar to a tokamak[1] in many ways. Like a tokamak, the plasma is confined by a combination of a toroidal magnetic field, B_ϕ, and a poloidal magnetic field, B_θ, in an axisymmetric toroidal configuration.[2] Unlike a tokamak, where $B_\phi \gg B_\theta$, the toroidal and poloidal field strengths are comparable, and the RFP toroidal field is largely generated by currents flowing within the plasma. The RFP concept derives its name from the fact that the toroidal magnetic field spontaneously reverses direction in the outer regions of the plasma. This reversal is a consequence of relaxation to a minimum energy state driven by intense magnetohydrodynamical (MHD) mode activity during the plasma start-up phase.[3] Intermittent, relatively low-level, mode activity maintains the reversal, by dynamo action, throughout the duration of the plasma discharge. As a magnetic fusion concept, the RFP has a number of possible advantages relative to the tokamak. The magnetic field strength at the coils is relatively low, allowing the possibility of a copper coil, as opposed to a superconducting-coil, reactor. Furthermore, the plasma current can, in principle, be increased sufficiently to allow Ohmic ignition, thus negating the need for auxiliary heating systems.

Unlike a tokamak, which can be completely MHD stable, a RFP is characterized by an ever present background level of MHD activity. The dominant MHD instabilities are rotating $m=1$ tearing modes with a range of toroidal modes numbers satisfying $n\epsilon_a \sim O(1)$. Here, m is the poloidal mode number, n is the toroidal mode number, $\epsilon_a = a/R_0$, and a and R_0 are the minor and major radii of the plasma, respectively. These modes, which are known as *dynamo modes*, since they are ultimately responsible for the dynamo action that maintains the field reversal, are generally resonant in the plasma core.

In the Madison Symmetric Torus (MST),[4,5] the dynamo modes continually execute a so-called *sawtooth cycle*, in which their typical amplitude gradually increases from a small value, until a critical value is reached at which a rapid global magnetic reconnection event, known as a *sawtooth crash*, is triggered. After the crash, the mode amplitudes return to their initial values, and the process continues *ad infinitum*. Note that the dynamo action that maintains the field reversal is only significant during the sawtooth crashes. This intermittency of the MHD dynamo is a common feature of RFPs.

It is often observed that in the early stages of the sawtooth cycle, well before the crash, the dynamo modes in a RFP become locked in phase to form a toroidally localized, rotating magnetic perturbation known as a ''slinky mode.''[6–8] This mode degrades the plasma confinement, giving rise to a rotating, toroidally localized ''hot spot'' on the plasma facing surface. Slinky modes sometimes lock to static error fields, and, thereby, stop rotating in the laboratory frame.[5,9] Unfortunately, when this occurs the associated ''hot spots'' also stop rotating and rapidly overheat the plasma facing surface, leading to the influx of impurities into the plasma, and the eventual termination of the discharge. Indeed, the plasma current in many RFPs [in particular, the Reversed-Field Experiment (RFX)[9,10]] is *limited* as a direct consequence of the problems associated with locked slinky modes.

The aim of this paper is to investigate the formation and locking of the slinky mode *analytically,* using techniques that have been employed, with considerable success, to investigate mode coupling and error-field related effects in tokamaks.[11–13] This is a complementary approach to that of using three-dimensional, nonlinear MHD simulations.[14,15]

In tokamaks, the dominant mode coupling mechanism is that due to toroidicity.[12] However, this coupling mechanism is far less important in RFPs, and is, in fact, neglected alto-

       1168

gether in this paper. The dominant mode coupling mechanism in RFPs is that due to the *nonlinear* interaction of different MHD modes inside the plasma.[16–18] Unfortunately, this type of coupling is far more difficult to analyze than the toroidal coupling that takes place inside tokamaks. In order to make any progress, it is necessary to *severely limit* the number of modes that are taken into account during the analysis. Hence, in this paper, only the intrinsically unstable $m=1$ tearing modes resonant in the plasma core, and the intrinsically stable 0,1 mode resonant at the reversal surface (where $B_\phi=0$) are taken into account, since these modes are judged to play the most significant roles in slinky mode formation and locking events. Note that all of the nonlinear coupling terms in this paper are calculated via *quasilinear* theory (i.e., using *liner* eigenfunctions—see Appendix A). This weakly nonlinear approach is justified during the sawtooth ramp phases, when the highly nonlinear MHD dynamo is not active, but obviously breaks down during the crashes. Indeed, it is easily checked that the nonlinear coupling terms obtained in this paper only represent small corrections to the linear stability of dynamo modes at the typical mode amplitudes required to trigger slinky formation.

There is another major difference between tokamaks and RFPs. Tokamaks generally possess intact, nested magnetic flux surfaces, except during major disruption events.[1] RFPs, on the other hand, only possess intact magnetic flux surfaces in the outer regions of the plasma, and even these flux surfaces are broken up during sawtooth crashes.[18] The magnetic field in the core of a RFP is *stochastic* in nature, due to the effect of overlapping magnetic islands associated with the dynamo modes. It follows that the nonlinear evolution of these modes cannot be analyzed using standard single-helicity magnetic island theory (i.e., Rutherford island theory[19]). In fact, the only assumption made in this paper regarding the nonlinear evolution of the dynamo modes is that these modes *saturate* at some level: this level increases gradually during a sawtooth ramp, and decreases abruptly at each sawtooth crash. On the other hand, both the linear and nonlinear evolution of the intrinsically stable 0,1 mode are analyzed using standard single-helicity theory. This approach is justified because the 0,1 rational surface (i.e., the reversal surface) usually lies in that region of the plasma possessing good magnetic flux surfaces.[18]

It is a standard MHD result[11] that 0,0 electromagnetic torques can only develop in those regions of the plasma where the linear equations of marginally stable ideal-MHD break down: i.e., in the layer or island regions centered on the various rational surfaces in the plasma. In this paper, the radial widths of these regions are neglected, so that the 0,0 torque takes the form of a series of radial δ functions, centered on the various rational surfaces. In reality, given the extensive island overlap that occurs in the plasma core, the radial distribution of the electromagnetic torque in the core is probably more continuous than this. However, this approximation is unlikely to be a source of significant error.

The plasma pressure is neglected in this paper for a number of reasons. First, finite plasma pressure greatly complicates the analysis of nonlinear mode coupling. Second, since the curvature of magnetic field lines is ''unfavorable'' in

RFPs, finite plasma pressure destabilizes resistive interchange modes,[20] which must then be taken into account during the analysis. Finally, and most importantly, plasma pressure is not thought to play a significant role in the formation and locking of slinky modes. Likewise, the finite resistivity of the flux conserving shell is not taken into account in this paper because resistive shell effects are also not thought to play an important role in the formation and locking of slinky modes.[15]

This paper is organized as follows. In Sec. II we investigate the formation of the slinky mode via the nonlinear coupling of multiple $m=1$ core tearing modes. The locking of the slinky mode to a static error field is examined in Sec. III. Finally, the main results of this paper are summarized in Sec. IV. The analysis of the nonlinear coupling between different MHD modes is described in detail in Appendix A. Likewise, the technical details of the analysis of error-field effects are contained in Appendix B.

II. FORMATION OF THE SLINKY MODE

A. Introduction

Consider a large aspect ratio,[21] zero-β,[22] circular cross section, RFP equilibrium. Suppose that R_0 and a are the major and minor radii of the plasma, respectively. The plasma is assumed to be surrounded by a concentric, close-fitting, perfectly conducting shell of minor radius b. In this paper, all calculations are carried out in *cylindrical* geometry, using the standard coordinates (r,θ,ϕ), where $\phi \equiv z/R_0$. The plasma equilibrium is described in more detail in Sec. A 1.

The m,n tearing mode is *resonant* inside the plasma at the m,n rational surface, minor radius $r_s^{m,n}$, which satisfies the resonance condition

$$F^{m,n}(r_s^{m,n})=0, \tag{1}$$

where $F^{m,n}(r)$ is given in Sec. A 3.

The radial magnetic perturbation associated with an m,n tearing mode is specified by the complex function $\psi^{m,n}(r,\theta,\phi,t)$ (see Sec. A 2), where

$$\psi^{m,n}(r,\theta,\phi,t)=\Psi^{m,n}(t)\hat{\psi}^{m,n}(r)e^{i(m\theta-n\phi)}. \tag{2}$$

Here, $\Psi^{m,n}$ is a complex constant that parametrizes the amplitude and phase of the perturbation at the rational surface, and $\hat{\psi}^{m,n}(r)$ is a real function that determines the variation of the perturbation amplitude across the plasma. These quantities are defined in more detail in Sec. A 3. Note that $\Psi^{m,n}$ is effectively the *reconnected magnetic flux* at the m,n rational surface.

It is helpful to write

$$\Psi^{m,n}(t)=\hat{\Psi}^{m,n}(t)e^{i\varphi^{m,n}}, \tag{3}$$

where $\hat{\Psi}^{m,n}\equiv|\Psi^{m,n}|$ and $\varphi^{m,n}\equiv\arg(\Psi^{m,n})$.

According to standard MHD theory, the magnetic perturbation associated with the m,n tearing mode *corotates* with the plasma at the associated rational surface.[11] In this paper, the plasma is assumed to rotate only in the *toroidal* direction, with angular velocity $\Omega(r,t)$. Thus,

$$\varphi^{m,n}(t)=\varphi_0^{m,n}+n\int_0^t \Omega(r_s^{m,n},t')dt'. \tag{4}$$

Consider the *nonlinear* coupling of the $1,n$ through $1,n+N-1$ tearing modes, which are generally resonant in the plasma *core*, via the $0,1$ mode, which is resonant at the *reversal surface*. The reversal surface (i.e., the surface at which the equilibrium toroidal magnetic field reverses direction) is usually located close to the plasma boundary. The $1,n$ through $1,n+N-1$ tearing modes are assumed to be intrinsically *unstable*, with saturated amplitudes $\hat{\Psi}^{1,n+j}$, for $j=0$ to $N-1$. On the other hand, the $0,1$ tearing mode is assumed to be intrinsically *stable*. Incidentally, N (i.e., the number of unstable $m=1$ tearing modes) is largely determined by the *inverse aspect ratio*, $\epsilon_a \equiv a/R_0$, of the device. Generally speaking, $N\epsilon_a \sim O(1)$. The conventional large aspect ratio RFP orderings are $\epsilon_a \ll 1$ and $n\epsilon_a \sim O(1)$.

B. Electromagnetic torques

Consider the nonlinear coupling of the $1,n+j$; $1,n+j+1$; and $0,1$ tearing modes, where j lies in the range 0 to

$N-2$. According to Eqs. (A94)–(A96), the nonlinear toroidal electromagnetic torques acting in the vicinity of the respective rational surfaces are written:

$$\delta T_{\phi\ \text{EM}}^{1,n+j}=-(n+j)T_{n+j}, \tag{5}$$

$$\delta T_{\phi\ \text{EM}}^{1,n+j+1}=(n+j+1)T_{n+j}, \tag{6}$$

$$\delta T_{\phi\ \text{EM}}^{0,1}=-T_{n+j}. \tag{7}$$

Equations (A100) and (A103) yield

$$T_{n+j}=-\frac{2\pi^2 R_0}{\mu_0}\frac{\text{Im}\{B^{0,1}(\Psi^{0,1})^*\}}{H^{0,1}(r_s^{0,1})}, \tag{8}$$

where

$$B^{0,1}=-(\Psi^{1,n+j})^*\Psi^{1,n+j+1}\frac{H^{0,1}(r_s^{0,1})}{4}\mathcal{P}\int_0^a t_{n+j}(r)dr, \tag{9}$$

and

$$t_{n+j}(r)=\sigma'\left\{r(\hat{\psi}^{1,n+j})'\hat{\psi}^{0,1}\hat{\psi}^{1,n+j+1}\frac{G^{1,n+j}}{H^{1,n+j}F^{0,1}F^{1,n+j+1}}+\hat{\psi}^{1,n+j}r(\hat{\psi}^{0,1})'\hat{\psi}^{1,n+j+1}\frac{G^{0,1}}{H^{0,1}F^{1,n+j}F^{1,n+j+1}}\right.$$
$$+\hat{\psi}^{1,n+j}\hat{\psi}^{0,1}r(\hat{\psi}^{1,n+j+1})'\frac{G^{1,n+j+1}}{H^{1,n+j+1}F^{1,n+j}F^{0,1}}+\hat{\psi}^{1,n+j}\hat{\psi}^{0,1}\hat{\psi}^{1,n+j+1}\left[r\sigma\left(\frac{F^{1,n+j}}{H^{1,n+j}F^{0,1}F^{1,n+j+1}}\right.\right.$$
$$\left.+\frac{F^{0,1}}{H^{0,1}F^{1,n+j}F^{1,n+j+1}}+\frac{F^{1,n+j+1}}{H^{1,n+j+1}F^{1,n+j}F^{0,1}}\right)+\frac{2B_\theta B_\phi-r\sigma(B_\theta^2+B_\phi^2)}{F^{1,n+j}F^{0,1}F^{1,n+j+1}}\left.\left.\right]\right\}. \tag{10}$$

Here, $\mathcal{P}$ denotes a Cauchy principal part, $'$ denotes d/dr, and the equilibrium functions $B_\theta(r)$, $B_\phi(r)$, $\sigma(r)$, $F^{m,n}(r)$, $G^{m,n}(r)$, and $H^{m,n}(r)$ are defined in Secs. A 1 and A 3.

The quantity $\Psi^{0,1}$ (i.e., the $0,1$ reconnected flux driven at the reversal surface by the nonlinear interaction of the $1,n+j$ and $1,n+j+1$ tearing modes) can be determined from *linear* layer physics. This approach is valid as long as the driven island width at the reversal surface is less than the linear layer width (see Sec. A 6 and Ref. 13). Equations (A32) and (A100) yield

$$\Delta^{0,1}(\omega_{n+j})\Psi^{0,1}\equiv\Delta\Psi^{0,1}=E^{0,1}\Psi^{0,1}+B^{0,1}. \tag{11}$$

Here, the real quantity $E^{0,1}$ (n.b., $E^{0,1}<0$) is the linear *tearing stability index* for the $0,1$ mode (see Sec. A 3), the complex quantity $\Delta^{0,1}$ is the *layer response function* for the $0,1$ mode (see Sec. A 5), and ω_{n+j} is the real frequency of the $0,1$ mode formed by the nonlinear interaction of the $1,n+j$ and $1,n+j+1$ modes, as seen in a frame of reference corotating with the plasma at the reversal surface. It follows that

$$\omega_{n+j}=(n+j)\Omega(r_s^{n+j})+\Omega(r_s^{0,1})-(n+j+1)\Omega(r_s^{n+j+1}). \tag{12}$$

In this paper, *poloidal* electromagnetic torques, and the modifications to the plasma poloidal rotation profile induced by such torques, are *neglected*. In general, poloidal electromagnetic torques are smaller than the corresponding toroidal torques by an inverse aspect ratio, $\epsilon_a=a/R_0$. On the other hand, the moment of inertia of the plasma is much smaller for poloidal rotation than for toroidal rotation. The net result is that the modifications to tearing mode frequencies induced by poloidal torques are of the same order of magnitude as those induced by toroidal torques. Thus, the neglect of poloidal torques is only justified if the plasma is subject to significant *poloidal flow damping*.[23] This is certainly the case in tokamaks. However, since flow damping is a toroidal effect (i.e., it does not occur in a cylinder), and toroidal effects tend to be far weaker in RFPs than in tokamaks, it is not obvious that flow damping is sufficiently strong in RFPs to justify the neglect of the poloidal torques. If the assumption of strong poloidal flow damping in RFPs (which greatly simplifies the analysis) turns out to be incorrect, the analysis presented in this paper can be generalized in a relatively straightforward manner to include the effect of the poloidal torques (see Ref. 11).

C. Viscous torques

The toroidal electromagnetic torques that develop in the plasma as a consequence of nonlinear mode coupling *modify* the plasma toroidal rotation profile. Such modifications are *opposed* by the action of (perpendicular) plasma viscosity. In *steady state*, the change induced in the toroidal angular velocity profile, $\Delta\Omega(r)$, satisfies

$$\frac{d}{dr}\left(r\mu\frac{d\Delta\Omega}{dr}\right)=0, \tag{13}$$

where $\mu(r)$ is the (anomalous) coefficient of (perpendicular) plasma viscosity. The plasma toroidal rotation is assumed to be ''clamped'' at the edge, so that

$$\Delta\Omega(a)=0. \tag{14}$$

Finally, the toroidal viscous torque that develops in the vicinity of the m,n rational surface takes the form

$$\delta T_{\phi\,\mathrm{VS}}^{m,n}=4\pi^2 R_0\left(r\mu R_0^2\frac{d\Delta\Omega}{dr}\right)_{r_{s-}^{m,n}}^{r_{s+}^{m,n}}. \tag{15}$$

Note that, like the electromagnetic torques, the steady-state viscous torques only develop in the vicinity of the rational surfaces. The assumptions underlying the analysis in this section are described in more detail in Ref. 11. Note, in particular, that it is possible to generalize the analysis to take account of the fact that tearing modes do not generally corotate with the ion fluid in RFPs without significantly modifying any of the results obtained in this paper.

D. Torque balance

In *steady state*, the electromagnetic torques that develop in the vicinity of the various coupled rational surfaces in the plasma must be balanced by viscous torques. Solving Eq.

(13) subject to the boundary condition (14), making use of Eqs. (5)–(7) and Eq. (15), including the electromagnetic torques generated at the reversal surface by *all* of the unstable $m=1$ tearing modes, and balancing the electromagnetic and viscous torques at *every* coupled rational surface, yields

$$\Omega_{n+j}=\Omega_{n+j}^{(0)}+\sum_{k=0}^{j-1}\left(\int_{r_{n+j}}^{r_*}\frac{\mu_*}{\mu}\frac{dr}{r}\right)\widetilde{T}_{n+k}$$
$$+\sum_{k=j}^{N-2}\left(\int_{r_{n+k+1}}^{r_*}\frac{\mu_*}{\mu}\frac{dr}{r}\right.$$
$$\left.-(n+k)\int_{r_{n+k}}^{r_{n+k+1}}\frac{\mu_*}{\mu}\frac{dr}{r}\right)\widetilde{T}_{n+k}, \tag{16}$$

for $j=0$ to $N-1$, where $\widetilde{T}_{n+k}=T_{n+k}/(4\pi^2 R_0^3\mu_*)$ and $\mu_* \equiv\mu(r_*)$. Here, $\Omega_{n+k}\equiv\Omega(r_s^{1,n+k})$. Likewise, $r_{n+k}\equiv r_s^{1,n+k}$ and $r_*\equiv r_s^{0,1}$. Also, $\Omega_{n+k}^{(0)}$ is the toroidal angular velocity of the plasma at radius $r_s^{1,n+k}$ in the *unperturbed* state. Of course, $\Delta\Omega(r_s^{1,n+k})\equiv\Omega_{n+k}-\Omega_{n+k}^{(0)}$. Note that the nonlinear electromagnetic torques *do not* modify the plasma rotation at the reversal surface.

Recall that

$$\omega_{n+j}=(n+j)\Omega_{n+j}+\Omega_*-(n+j+1)\Omega_{n+j+1} \tag{17}$$

[where $\Omega_*\equiv\Omega(r_*)$ is the plasma angular velocity at the reversal surface] is the real frequency of the 0,1 mode formed by the nonlinear coupling of the $1,n+j$ and $1,n+j+1$ tearing modes, as seen in a frame corotating with the plasma at the reversal surface. Of course,

$$\omega_{n+j}^{(0)}=(n+j)\Omega_{n+j}^{(0)}+\Omega_*-(n+j+1)\Omega_{n+j+1}^{(0)} \tag{18}$$

is the value of ω_{n+j} in the unperturbed plasma. Equations (16)–(18) can be combined to give the following set of coupled torque balance equations:

$$\omega_{n+j}-\omega_{n+j}^{(0)}=(n+j)\sum_{k=0}^{j-1}\left(\int_{r_{n+j}}^{r_*}\frac{\mu_*}{\mu}\frac{dr}{r}\right)\widetilde{T}_{n+k}-(n+j+1)\sum_{k=0}^{j}\left(\int_{r_{n+j+1}}^{r_*}\frac{\mu_*}{\mu}\frac{dr}{r}\right)\widetilde{T}_{n+k}$$
$$+(n+j)\sum_{k=j}^{N-2}\left(\int_{r_{n+k+1}}^{r_*}\frac{\mu_*}{\mu}\frac{dr}{r}-(n+k)\int_{r_{n+k}}^{r_{n+k+1}}\frac{\mu_*}{\mu}\frac{dr}{r}\right)\widetilde{T}_{n+k}$$
$$-(n+j+1)\sum_{k=j+1}^{N-2}\left(\int_{r_{n+k+1}}^{r_*}\frac{\mu_*}{\mu}\frac{dr}{r}-(n+k)\int_{r_{n+k}}^{r_{n+k+1}}\frac{\mu_*}{\mu}\frac{dr}{r}\right)\widetilde{T}_{n+k}, \tag{19}$$

for $j=0$ to $N-2$.

E. Two unstable $m=1$ tearing modes: $N=2$

1. Basic equations

Suppose that only the $1,n$ and $1,n+1$ tearing modes are intrinsically unstable: i.e., $N=2$. Equations (16)–(19) yield the torque balance equation,

$$\omega_n^{(0)}-\omega_n=L_n\widetilde{T}_n(\omega_n), \tag{20}$$

plus

$$\Omega_n-\Omega_n^{(0)}=M_n\widetilde{T}_n(\omega_n), \tag{21}$$

$$\Omega_{n+1}-\Omega_{n+1}^{(0)}=N_{n+1}\widetilde{T}_n(\omega_n), \tag{22}$$

where

$$\omega_n=n\Omega_n+\Omega_*-(n+1)\Omega_{n+1}, \tag{23}$$

$$\omega_n^{(0)}=n\Omega_n^{(0)}+\Omega_*-(n+1)\Omega_{n+1}^{(0)}. \tag{24}$$

Here,

$$L_n = n^2 \int_{r_n}^{r_{n+1}} \frac{\mu_*}{\mu} \frac{dr}{r} + \int_{r_{n+1}}^{r_*} \frac{\mu_*}{\mu} \frac{dr}{r}, \tag{25}$$

$$M_n = \int_{r_{n+1}}^{r_*} \frac{\mu_*}{\mu} \frac{dr}{r} - n \int_{r_n}^{r_{n+1}} \frac{\mu_*}{\mu} \frac{dr}{r}, \tag{26}$$

$$N_n = \int_{r_n}^{r_*} \frac{\mu_*}{\mu} \frac{dr}{r}. \tag{27}$$

2. Linear analysis

Equations (8), (9), and (11) can be rearranged to give

$$\tilde{T}_n = -\frac{1}{2} \frac{\tau_V}{\tau_H^2} \chi_n^2 \frac{\mathrm{Im}[\Delta^{0,1}(\omega_n)]}{|\Delta^{0,1}(\omega_n) - E^{0,1}|^2}, \tag{28}$$

where

$$\tau_H = \left(\frac{\mu_0 \rho_*}{(F'_*)^2} \right)^{1/2}, \tag{29}$$

$$\tau_V = \frac{\rho_* r_*^2}{\mu_*}, \tag{30}$$

$$\chi_n = |P_n| \tilde{\Psi}^{1,n} \tilde{\Psi}^{1,n+1}, \tag{31}$$

$$P_n = -\frac{\epsilon_*^2 r_*^2 F'_*}{4} \mathcal{P} \int_0^a t_n(r) dr, \tag{32}$$

$$\epsilon_* = \frac{r_*}{R_0}, \tag{33}$$

$$F'_* = d[F^{0,1}(r_*)]/dr, \tag{34}$$

$$\tilde{\Psi}^{1,n} = \frac{\hat{\Psi}^{1,n}}{r_*^2 F'_*}, \tag{35}$$

$$\tilde{\Psi}^{1,n+1} = \frac{\hat{\Psi}^{1,n+1}}{r_*^2 F'_*}. \tag{36}$$

Here, ρ_* is the plasma mass density at the reversal surface, τ_H and τ_V are the hydromagnetic and viscous time scales evaluated at the reversal surface, respectively, and χ_n, P_n, $\tilde{\Psi}^{1,n}$, and $\tilde{\Psi}^{1,n+1}$ are nondimensional real constants.

According to Sec. A 5, in the so-called *viscoresistive* regime (i.e., the most appropriate linear response regime for an Ohmically heated device[13]), the layer response function for the 0,1 mode takes the form

$$\Delta^{0,1}(\omega_n) = -i \omega_n \tau_*, \tag{37}$$

where

$$\tau_* = 2.104 \frac{\tau_H^{1/3} \tau_R^{5/6}}{\tau_V^{1/6}} \tag{38}$$

is the L/R time of the resistive layer driven at the reversal surface by the nonlinear coupling of the $1,n$ and $1,n+1$ tearing modes. Here,

$$\tau_R = \frac{\mu_0 r_*^2}{\eta_*} \tag{39}$$

is the resistive diffusion time scale, evaluated at the reversal surface, and η_* is the plasma (parallel) resistivity at radius r_*.

Equations (20), (28), and (37) can be combined to give the normalized torque balance equation,

$$\frac{1}{4} \frac{\chi_n^2}{\Lambda_n^2} \frac{\hat{\omega}_n}{\zeta_n^2 + \hat{\omega}_n^2} = 1 - \hat{\omega}_n, \tag{40}$$

where

$$\hat{\omega}_n = \frac{\omega_n}{\omega_n^{(0)}}, \tag{41}$$

$$\zeta_n = \frac{-E^{0,1}}{\omega_n^{(0)} \tau_*}, \tag{42}$$

$$\Lambda_n^2 = \frac{1}{2} \frac{[\omega_n^{(0)}]^2 \tau_* \tau_H^2}{\tau_V} \Big/ L_n. \tag{43}$$

Equation (40) is very similar to the torque balance equation that governs the behavior of a conventional induction motor.[24] Furthermore, Eq. (40) is exactly analogous to the torque balance equation which governs the locking of a rotating tearing mode to an error field,[11,25] and also the equation that governs the locking of two toroidally coupled, differentially rotating, tearing modes in a tokamak.[12,26]

It is easily demonstrated that if $\zeta_n > 1/\sqrt{27}$, then Eq. (40) possesses *continuous* solutions, whereas if $\zeta_n < 1/\sqrt{27}$ then the solutions split into *two* separate branches. In a RFP (as in a tokamak[11]) it is generally expected that $\zeta_n \ll 1$ [since the plasma rotation period is generally much less than the L/R time of a resistive layer—see Eq. (42)].

In the physically relevant limit $\zeta_n \ll 1$, the two branches of solutions to Eq. (40) are as follows. On the *unlocked* branch, which is characterized by $\omega_n \sim \omega_n^{(0)}$, Eq. (40) reduces to

$$\omega_n = \frac{\omega_n^{(0)}}{2} \left(1 + \sqrt{1 - \frac{\chi_n^2}{\Lambda_n^2}} \right), \tag{44}$$

whereas on the *locked* branch, which is characterized by $\omega_n \sim \zeta_n \omega_n^{(0)}$, Eq. (40) yields

$$\omega_n = \frac{\omega_n^{(0)}}{8} \left(\frac{\chi_n^2}{\Lambda_n^2} - \sqrt{\frac{\chi_n^4}{\Lambda_n^4} - 64 \zeta_n^2} \right). \tag{45}$$

Note that the *unlocked* branch of solutions ceases to exist for

$$\chi_n \gtrsim \Lambda_n. \tag{46}$$

When the ''amplitude'' of the two coupled tearing modes (i.e., χ_n) exceeds the critical value given above, a bifurcation from the unlocked to the locked branch of solutions takes place. Such a bifurcation is termed a *locking bifurcation*. Note, also, that the *locked* branch of solutions ceases to exist for

$$\chi_n \lesssim (8\zeta_n)^{1/2} \Lambda_n. \tag{47}$$

When the mode amplitude falls below the critical value given above, a bifurcation from the locked to the unlocked branch of solutions takes place. Such a bifurcation is termed
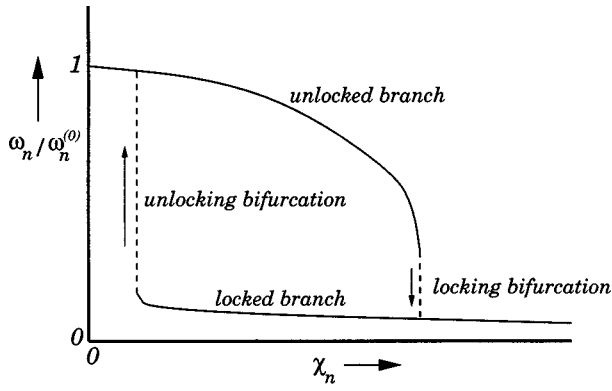
FIG. 1. The bifurcation diagram for the formation and breakup of the slinky mode. All quantities are defined in Sec. II E 2.

3. Nonlinear analysis

Equation (40) was derived using *linear* layer physics to calculate the 0,1 reconnected flux driven at the reversal surface by the nonlinear interaction of the 1,n and 1,$n+1$ tearing modes. As discussed in Ref. 13, this approach is generally appropriate on the unlocked branch of solutions, where ω_n is large, since driven magnetic reconnection at the reversal surface is effectively suppressed by differential plasma rotation (parametrized by ω_n). On the other hand, there is no suppression of magnetic reconnection on the locked branch of solutions, where ω_n is small, so the system can be expected to enter the *nonlinear* regime once locking has taken place. Note that the locking threshold, Eq. (46), is not modified by nonlinear effects, since this threshold only depends on the properties of the unlocked branch of solutions. However, in general, the unlocking threshold, Eq. (47), *is* modified by nonlinear effects. The nonlinear regime is characterized by the presence of a chain of driven magnetic islands at the reversal surface. The plasma in the vicinity of the reversal surface cannot flow across the magnetic separatrix associated with this island chain, so in the nonlinear regime there arises a *no-slip* constraint, which demands that the driven island chain at the reversal surface must *corotate exactly* with the plasma at this surface.[11,13] The no-slip constraint gives

$$\omega_n \equiv n\Omega_n + \Omega_* - (n+1)\Omega_{n+1} = 0, \qquad (48)$$

on the locked branch of solutions.

On the locked branch of solutions, the 0, 1 reconnected flux driven at the reversal surface by the nonlinear interaction of the 1,n and 1,$n+1$ tearing modes is determined by the Rutherford island equation, (A37), which yields

$$4I\tau_R \frac{d(\sqrt{\tilde{\Psi}^{0,1}})}{dt} = \mathrm{Re}\left(\frac{\Delta\Psi^{0,1}}{\Psi^{0,1}}\right) = E^{0,1} + \frac{\chi_n}{\tilde{\Psi}^{0,1}}\cos\Delta\varphi_n, \qquad (49)$$

where $I = 0.8227$. Here, $4\sqrt{\tilde{\Psi}^{0,1}}r_*$ is the radial width of the island chain driven at the reversal surface, $\tilde{\Psi}^{0,1} = \tilde{\Psi}^{0,1}/r_*^2 F_*'$,

$$\Delta\varphi_n = \varphi_0^{1,n} + \varphi_0^{0,1} - \varphi_0^{1,n+1} + [1 - \mathrm{sgn}(P_n)]\frac{\pi}{2}, \qquad (50)$$

and use has been made of Eq. (48). Of course, $\mathrm{sgn}(P_n) = \pm 1$ as $P_n \gtrless 0$.

The torque balance equation (20) reduces to

$$\omega_n^{(0)} = L_n\tilde{T}_n = \frac{L_n}{2}\frac{\tau_V}{\tau_H^2}\chi_n\tilde{\Psi}^{0,1}\sin\Delta\varphi_n, \qquad (51)$$

on the locked branch of solutions. It is easily demonstrated that all solutions characterized by $|\Delta\varphi_n| > \pi/2$ are *dynamically unstable*.[11]

In steady state, Eqs. (49) and (51) yield

$$\tilde{\Psi}^{0,1} = \frac{\chi_n}{-E^{0,1}}\cos\Delta\varphi_n, \qquad (52)$$

and

$$8\zeta_n\Lambda_n^2 = \chi_n^2\sin 2\Delta\varphi_n. \qquad (53)$$

Note that the locked branch of solutions ceases to exist for

$$\chi_n \leq (8\zeta_n)^{1/2}\Lambda_n. \qquad (54)$$

When the mode amplitude, χ_n, falls below this critical value an unlocking bifurcation takes place. In this simple example, the unlocking threshold (54) predicted by nonlinear theory is the same as the threshold (47) predicted by linear theory. In general, however, this is not the case, and the correct unlocking threshold is that predicted by *nonlinear* theory.

Note, finally, that in the *strongly locked* limit, in which the mode amplitude lies well above the unlocking threshold, Eq. (53) gives

$$\Delta\varphi_n \simeq 0. \qquad (55)$$

4. Mode structure

In order to understand the significance of the constraint $\omega_n = 0$, which characterizes the locked branch of solutions, it is necessary to calculate the plasma angular velocities at the 1,n and 1,$n+1$ rational surfaces after locking. Equation (20)–(22) yield

$$n\Omega_n = \omega_0, \qquad (56)$$

$$(n+1)\Omega_{n+1} = \omega_0 + \Omega_*, \qquad (57)$$

on the locked branch of solutions, where

$$\omega_0 = n\left(\Omega_n^{(0)} + \frac{M_n}{L_n}\omega_n^{(0)}\right). \qquad (58)$$

The above expressions suggest that locking is associated with a *slight* redistribution of the plasma toroidal angular momentum interior to the reversal surface (since $\omega_n^{(0)}$

$\sim\Omega_n^{(0)}\sim\Omega_{n+1}^{(0)}$ and $L_n\sim nM_n$). In other words, the locking process is *not*, in general, associated with a dramatic change in the core plasma rotation.

According to Eqs. (2) and (3), the radial magnetic perturbation associated with the saturated $1,n$ and $1,n+1$ tearing modes resonant in the plasma core is characterized by

$$\psi(r,\theta,\phi,t)=\hat{\Psi}^{1,n}\hat{\psi}^{1,n}(r)e^{i[\theta-n\phi+\varphi_0^{1,n}+n\Omega_n t]}$$
$$+\hat{\Psi}^{1,n+1}\hat{\psi}^{1,n+1}(r)$$
$$\times e^{i[\theta-(n+1)\phi+\varphi_0^{1,n+1}+(n+1)\Omega_{n+1}t]}. \quad (59)$$

Here, the contribution of the nonlinearly driven $0,1$ mode is neglected, since $\hat{\Psi}^{0,1}\ll\hat{\Psi}^{1,n},\hat{\Psi}^{1,n+1}$. On the *locked* branch of solutions, the above expression reduces to

$$\psi(r,\theta,\phi,t)=\{A_n(r)+A_{n+1}(r)e^{-i\varphi_*(\phi,t)}\}$$
$$\times e^{i(\theta-n\phi+\varphi_0^{1,n}+\omega_0 t)}, \quad (60)$$

where

$$A_n(r)=\hat{\Psi}^{1,n}\hat{\psi}^{1,n}(r), \quad (61)$$

$$A_{n+1}(r)=\text{sgn}(P_n)\hat{\Psi}^{1,n+1}\hat{\psi}^{1,n+1}(r), \quad (62)$$

$$\varphi_*(\phi,t)=\phi-\varphi_0^{0,1}-\Omega_* t, \quad (63)$$

and use has been made of Eqs. (48) and (55)–(57). Here, it is assumed that the mode amplitude lies well above the unlocking threshold. It follows that

$$|\psi(r,\theta,\phi,t)|=\{A_n^2+A_{n+1}^2+2A_nA_{n+1}\cos\varphi_*\}^{1/2}. \quad (64)$$

Note that the amplitude of the perturbed radial magnetic field possesses an $n=1$ modulation that corotates with the plasma at the reversal surface [see Eq. (63)]. Within this relatively slowly rotating $n=1$ envelope, the field exhibits high-n, high-frequency oscillations (assuming, as seems reasonable, that the plasma core rotates far more rapidly than the plasma at the reversal surface). Admittedly, the amplitude of the radial magnetic perturbation also exhibits an $n=1$ modulation on the unlocked branch of solutions. However, this modulation rotates at an angular velocity, which is, in general, not related to the angular velocity of the plasma at the reversal surface. Clearly, the only difference between the locked and unlocked branches of solutions is that the $n=1$ modulation is forced to corotate with the plasma at the reversal surface on the former branch of solutions, but is free to rotate with any angular velocity on the latter branch. However, as will soon become apparent, when there are more than two unstable $m=1$ tearing modes resonant in the plasma core the distinction between the unlocked and locked branches of solutions becomes far more significant.

F. Many unstable $m=1$ tearing modes: $N>2$

1. Basic equations

Suppose that all of the $1,n+j$ tearing modes are intrinsically unstable, where $j=0$, $N-1$, and $N>2$. Equations (16)–(19) yield the coupled torque balance equations,

$$\omega_{n+j}^{(0)}-\omega_{n+j}=\sum_{k=0}^{j-1}M_{n+j}\tilde{T}_{n+k}+L_{n+j}\tilde{T}_{n+j}$$
$$+\sum_{k=j+1}^{N-2}M_{n+k}\tilde{T}_{n+k}, \quad (65)$$

for $j=0$, $N-2$, plus

$$\Omega_{n+j}-\Omega_{n+j}^{(0)}=\sum_{k=0}^{j-1}N_{n+j}\tilde{T}_{n+k}+\sum_{k=j}^{N-2}M_{n+k}\tilde{T}_{n+k}, \quad (66)$$

for $j=0$, $N-1$.

2. Linear analysis

On the unlocked branch of solutions, where linear analysis remains valid, the coupled torque balance equations reduce to

$$1-\hat{\omega}_{n+j}=\frac{1}{4}\left(\sum_{k=0}^{j-1}\lambda_{n+k,n+j}\frac{\chi_{n+k}^2}{\Lambda_{n+k}^2\hat{\omega}_{n+k}}+\frac{\chi_{n+j}^2}{\Lambda_{n+j}^2\hat{\omega}_{n+j}}\right.$$
$$\left.+\sum_{k=j+1}^{N-2}\kappa_{n+j,n+k}\frac{\chi_{n+k}^2}{\Lambda_{n+k}^2\hat{\omega}_{n+k}}\right), \quad (67)$$

for $j=0$, $N-2$. Here,

$$\kappa_{n,n'}=\frac{M_{n'}}{L_{n'}}\frac{\omega_{n'}^{(0)}}{\omega_n^{(0)}}, \quad (68)$$

$$\lambda_{n,n'}=\frac{M_{n'}}{L_n}\frac{\omega_n^{(0)}}{\omega_{n'}^{(0)}}. \quad (69)$$

Equation (67) can only be solved analytically for the $\hat{\omega}_{n+j}$ when $N<4$.[25] However, the numerical solution of these equations is fairly straightforward. A locking bifurcation is indicated by the sudden disappearance of the physical root of Eq. (67) as the mode amplitudes, χ_{n+j}, are gradually increased. If the $1,n+l$ and $1,n+l+1$ modes are locked (where l lies in the range 0, $N-2$), but the remaining modes are unlocked, then Eq. (67) are modified by allowing $\hat{\omega}_{n+l}\to 0$ while $\chi_{n+l}^2/\hat{\omega}_{n+l}$ remains finite. In this manner, it is possible to obtain the equations governing the further locking of *any* combination of locked and unlocked $m=1$ modes.

3. Nonlinear analysis

Consider the *fully locked* state, in which the $1,n$ to $1,n+N-1$ modes are all locked together. It follows that

$$\omega_{n+j}=0, \quad (70)$$

for $j=0$, $N-2$. In steady state, the Rutherford island equation, (A37), gives

$$\tilde{\Psi}^{0,1}=\frac{\sum_{j=0}^{N-2}\chi_{n+j}\cos\Delta\varphi_{n+j}}{-E^{0,1}}, \quad (71)$$

where χ_n and $\Delta\varphi_n$ are defined in Eqs. (31) and (50), respectively. The above expression can be combined with the torque balance equations (65) to give

$$1 = \frac{1}{4} \left(\sum_{j=0}^{N-2} \chi_{n+j} \cos \Delta \varphi_{n+j} \right)$$

$$\times \left(\sum_{k=0}^{j-1} \lambda_{n+k,n+j} \frac{\chi_{n+k}}{\zeta_{n+k} \Lambda_{n+k}^2} \sin \Delta \varphi_{n+k} \right.$$

$$+ \frac{\chi_{n+j}}{\zeta_{n+j} \Lambda_{n+j}^2} \sin \Delta \varphi_{n+j}$$

$$\left. + \sum_{k=j+1}^{N-2} \kappa_{n+j,n+k} \frac{\chi_{n+k}}{\zeta_{n+k} \Lambda_{n+k}^2} \sin \Delta \varphi_{n+k} \right), \quad (72)$$

for $j = 0, N-2$. Equation (72) can only be solved analytically for the $\Delta \varphi_{n+j}$ when $N < 3$. However, the numerical solution of these equations is fairly straightforward. An unlocking bifurcation is indicated by the sudden disappearance of the physical root of Eq. (72) as the mode amplitudes, χ_{n+j}, are gradually decreased. If the $1, n+l$ mode unlocks (where l lies in the range $1, N-2$), but the other modes remain locked, then Eq. (72) are modified by neglecting the equations corresponding to $j = l-1$ and $j = l$, and letting χ_{n+l-1}, $\chi_{n+l} \to 0$ in the remaining equations. If the $1, n$ mode unlocks, but the other modes remain locked, then Eq. (72) are modified by neglecting the first equation, and letting $\chi_n \to 0$ in the remaining equations. Finally, if the $1, n+N-1$ mode unlocks, but the other modes remain locked, then Eq. (72) are modified by neglecting the last equation, and letting $\chi_{n+N-2} \to 0$ in the remaining equations. In this manner, it is possible to obtain the equations governing the further unlocking of *any* combination of locked and unlocked $m = 1$ modes.

Note that in the strongly locked limit, in which the mode amplitudes lie well above the unlocking threshold, Eq. (72) yield

$$\Delta \varphi_{n+j} \simeq 0, \quad (73)$$

for $j = 0, N-2$.

4. Mode structure

According to Eqs. (65) and (66), in the fully locked state the angular velocities of the plasma at the various coupled $m = 1$ rational surfaces are given by

$$(n+j) \Omega_{n+j} = \omega_0 + j \Omega_*, \quad (74)$$

for $j = 0, N-1$. Here,

$$\omega_0 = n \left(\Omega_n^{(0)} + \sum_{j,k=0}^{N-2} M_{n+j} (\mathbf{M}^{-1})_{j,k} \omega_{n+k}^{(0)} \right), \quad (75)$$

where

$$\mathbf{M}_{j,k} = \begin{cases} M_{n+k}, & \text{for } j < k, \\ L_{n+j}, & \text{for } j = k, \\ M_{n+j}, & \text{for } j > k, \end{cases} \quad (76)$$

for j, k in the range 0 to $N-2$. Again, it is clear that locking is, in general, associated with a *slight* redistribution of the plasma toroidal angular momentum interior to the reversal surface (since $\omega_{n+j}^{(0)} \sim \Omega_{n+k}^{(0)}$ and $L_{n+j} \sim n M_{n+k}$).

The radial magnetic perturbation associated with the fully locked state is characterized by

$$\psi(r, \theta, \phi, t) = \left\{ \sum_{j=0}^{N-1} A_{n+j} e^{-ij\varphi_*} \right\} e^{i(\theta - n\phi + \varphi_0^{1,n} + \omega_0 t)}, \quad (77)$$

where use has been made of Eqs. (70), (73), and (74). Here, it is assumed that the mode amplitudes lie well above the unlocking threshold. The A_n and φ_* are defined in Eqs. (61) and (63), respectively. Furthermore,

$$A_{n+j}(r) = \left(\prod_{k=0}^{j-1} \text{sgn}(P_{n+k}) \right) \hat{\Psi}^{1,n+j} \hat{\psi}^{1,n+j}(r), \quad (78)$$

for $j = 1, N-1$. It follows that

$$|\psi(r, \theta, \phi, t)| = \left(\sum_{j,k=0}^{N-1} A_{n+j} A_{n+k} \cos[(j-k) \varphi_*] \right)^{1/2}. \quad (79)$$

Note that the amplitude of the perturbed radial magnetic field possesses a toroidal modulation that corotates with the plasma at the reversal surface [see Eq. (63)]. Within this relatively slowly rotating envelope, the field exhibits high-n, high-frequency oscillations (assuming, again, that the plasma core rotates far more rapidly than the plasma at the reversal surface). The N coupled $m = 1$ modes add *coherently*, so that

$$|\psi| = \left| \sum_{j=0}^{N-1} A_{n+j} \right|, \quad (80)$$

at a single toroidal angle, specified by $\varphi_* = 0$, which also corotates with the plasma at the reversal surface. In general, if the modes are unlocked, or only partially locked, then they add *incoherently* throughout the plasma, so that

$$|\psi| \simeq \sqrt{\sum_{j=0}^{N-1} A_{n+j}^2}. \quad (81)$$

Thus, the peak mode amplitude in the fully locked state is roughly $\sqrt{N}$ times that in the unlocked state.

The structure of the slowly rotating envelope that characterizes the fully locked state can be elucidated by making the simplifying assumption that $A_{n+j} = A_n$ for $j = 0, N-1$. In this case,

$$|\psi(r, \theta, \phi, t)| = A_n \sqrt{\frac{1 - \cos N\varphi_*}{1 - \cos \varphi_*}}. \quad (82)$$

As illustrated in Fig. 2, there is a single primary maximum, located at $\varphi_* = 0$, at which $|\psi| = N A_n$. There are $N-1$ minima, located at $\varphi_* = j 2\pi/N$, for $j = 1, N-1$, at which $|\psi| = 0$. Finally, there are $N-2$ secondary maxima, located at $\varphi_* \simeq (2j-1)\pi/N$, for $j = 2, N-1$, at which $|\psi| \sim A_n$. The angular width of the primary maximum is $4\pi/N$.

It is clear that in situations where there are many unstable $m = 1$ tearing modes, resonant in the plasma core, mode locking gives rise to the formation of a *toroidally localized, coherent, interference pattern* in the perturbed magnetic field, which corotates with the plasma at the reversal surface. The toroidal angular width of this interference pattern is determined solely by the number of locked $m = 1$
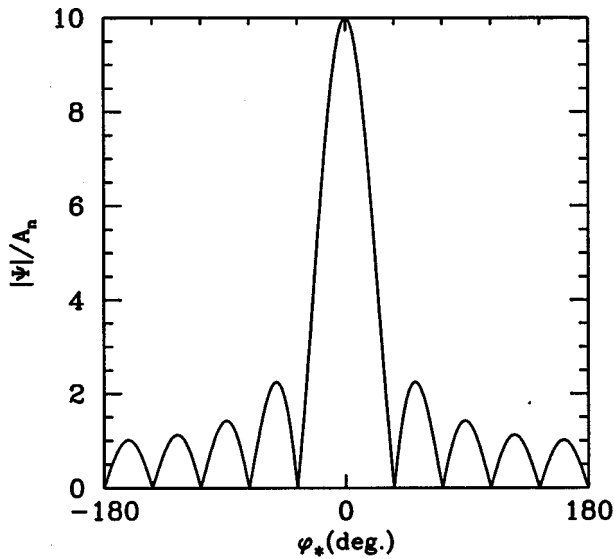
FIG. 2. The amplitude of the perturbed radial magnetic field plotted as a function of the toroidal angle for a typical slinky mode made up of ten nonlinearly coupled $m=1$ core tearing modes of equal amplitude. All quantities are defined in Sec. II F 4.

modes. The interference pattern forms a relatively slowly rotating envelope within which the magnetic field exhibits high-n, high-frequency oscillations (assuming, as seems reasonable, that the plasma core rotates far more rapidly than the plasma at the reversal surface). The nature of these high-frequency oscillations is determined by the core plasma rotation, as well as the toroidal mode numbers of the constituent $m=1$ tearing modes. Note, in particular, that the occurrence of a slowly rotating magnetic interference pattern *does not* necessarily imply that the plasma core is slowly rotating.

The magnetic interference pattern described above is identified with the so-called ''slinky mode,'' which has been observed both experimentally[6–8] and in numerical simulations.[14,15]

G. Effect of enhanced core viscosity

1. Introduction

In the above analysis, it is tacitly assumed that the (anomalous) perpendicular viscosity in the plasma core is not dramatically different to that in the vicinity of the reversal surface. In reality, the dominant contribution to the radial momentum transport in a RFP comes from free streaming along stochastic magnetic field lines generated by the overlapping $m=1$ magnetic island chains in the plasma core.[27,28] However, the magnetic field is not generally expected to be stochastic in the outer regions of the plasma (except during sawtooth relaxation events).[18] Hence, it is probable that the viscosity in the plasma core is significantly *enhanced*, due to the presence of the saturated $m=1$ tearing modes, with respect to that at the reversal surface. In order to more fully understand the effect of such an enhancement on the formation of the slinky mode, this section considers an *extreme* case in which the viscosity in the plasma core is taken to be *infinite*. To be more exact, $\mu(r)$ is assumed to be infinite in

the region $r < r_c$, where $r_{n+N-1} < r_c < r_*$. Of course, the viscosity is assumed to be finite in the region $r_c < r < a$. As before, the N unstable $m=1$ tearing modes have toroidal mode numbers in the range n to $n+N-1$.

Since the viscosity in the plasma core is effectively infinite, it is only sensible to assume that in the unperturbed state the plasma core rotates toroidally as a *rigid body*. It follows that

$$\Omega_{n+j}^{(0)} = \Omega_n^{(0)}, \tag{83}$$

for $j=0, N-1$. Furthermore,

$$\omega_{n+j}^{(0)} = \omega_n^{(0)}, \tag{84}$$

for $j=1, N-2$, where

$$\omega_n^{(0)} = \Omega_* - \Omega_n^{(0)}. \tag{85}$$

For the case of infinite core viscosity, Eqs. (25)–(27) reduce to

$$L_{n+j} = M_{n+j} = L_c, \tag{86}$$

for $j=0, N-2$, and

$$N_{n+j} = L_c, \tag{87}$$

for $j=1, N-1$, where

$$L_c = \int_{r_c}^{r_*} \frac{\mu_*}{\mu} \frac{dr}{r}. \tag{88}$$

Thus, Eqs. (28) and (66) imply that

$$\Omega_{n+j} = \Omega_n, \tag{89}$$

for $j=1, N-1$: i.e., the plasma core continues to rotate toroidally as a rigid body in the presence of nonlinear electromagnetic torques. Furthermore,

$$\omega_{n+j} = \omega_n, \tag{90}$$

for $j=0, N-2$, where

$$\omega_n = \Omega_* - \Omega_n. \tag{91}$$

2. Linear analysis

In the presence of a strongly enhanced core viscosity, the $N-1$ torque balance equations (67) become identical. It follows that the unlocked branch of solutions is governed by a single torque balance equation of the form

$$\hat{\omega}_n(1 - \hat{\omega}_n) = \frac{1}{4\Lambda_c^2} \sum_{j=0}^{N-2} \chi_{n+j}^2, \tag{92}$$

where $\hat{\omega}_n$ is defined in Eq. (41), and

$$\Lambda_c^2 = \frac{1}{2} \frac{[\omega_n^{(0)}]^2 \tau_* \tau_H^2}{\tau_V} \bigg/ L_c. \tag{93}$$

The core plasma rotation velocity, Ω_n, is related to ω_n via

$$\Omega_n = \Omega_* - \omega_n. \tag{94}$$

According to Eq. (92), the unlocked branch of solutions ceases to exist for

$$\sum_{j=0}^{N-2} \chi_{n+j}^2 \geq \Lambda_c^2. \tag{95}$$

When the left-hand side of the above expression exceeds the right-hand side, a bifurcation takes place in which the $1,n$ through $1,n+N-1$ core tearing modes *simultaneously* lock together. Of course, $\omega_n = 0$ in the locked state. The great simplification of simultaneous, as opposed to piecemeal, locking occurs because the enhanced core viscosity forces the $m = 1$ tearing modes resonant in the plasma core to rotate toroidally with the same *phase velocity*.

Note that the locking threshold (95) only depends on the unenhanced plasma viscosity in the outer regions of the plasma [through the parameter L_c—see Eq. (88)].

3. Nonlinear analysis

Consider the locked branch of solutions, on which $\omega_n = 0$. In the presence of strongly enhanced core viscosity, the $N-1$ torque balance equations (72) yield

$$\Delta\varphi_{n+j} = \Delta\varphi_n, \tag{96}$$

for $j=0, N-2$. It follows that the locked branch of solutions is governed by a single torque balance equation of the form

$$8\zeta_n \Lambda_c^2 = \left(\sum_{j=0}^{N-2} \chi_{n+j}\right)^2 \sin 2\Delta\varphi_n, \tag{97}$$

where ζ_n is defined in Eq. (42).

According to Eq. (97), the locked branch of solutions ceases to exist for

$$\left(\sum_{j=0}^{N-2} \chi_{n+j}\right)^2 \leq 8\zeta_n \Lambda_c^2. \tag{98}$$

When the right-hand side of the above expression exceeds the left-hand side, a bifurcation takes place in which the $1,n$ through $1,n+N-1$ core tearing modes *simultaneously* unlock. As usual, there is strong hysteresis in the locking/unlocking process, since the locking threshold (95) is much less than the unlocking threshold (98) when both are expressed in terms of the typical amplitude of a saturated $m = 1$ tearing mode in the plasma core.

Note that the unlocking threshold (98) also only depends on the unenhanced plasma viscosity in the outer regions of the plasma [through the parameter L_c—see Eq. (88)].

In the strongly locked limit, in which the left-hand side of Eq. (98) greatly exceeds the right-hand side, the torque balance equation (97) yields

$$\Delta\varphi_n \simeq 0. \tag{99}$$

4. Mode structure

On the locked branch of solutions, where $\omega_n = 0$, Eq. (94) gives

$$\Omega_n = \Omega_*: \tag{100}$$

i.e., after locking, the whole plasma core corotates with the plasma at the reversal surface. Clearly, in marked contrast to the cases discussed previously, mode locking in the presence of enhanced core viscosity is associated with a *significant*

reduction in the toroidal angular momentum of the plasma interior to the reversal surface (assuming that the plasma core is initially rotating much faster than the outer regions of the plasma).

The radial magnetic perturbation associated with the N saturated $m = 1$ tearing modes in the plasma core is specified by

$$\psi(r,\theta,\phi,t) = \left(\sum_{j=0}^{N-1} A_{n+j}(r) e^{-i(j\phi - \varphi_0^{1,n+j} - j\Omega_n t)}\right)$$
$$\times e^{i(\theta - n\phi + n\Omega_n t)}, \tag{101}$$

where the $A_{n+j}(r)$ are defined in Eqs. (61) and (78), and use has been made of Eq. (89). Note that on the unlocked branch of solutions the modes *do not*, in general, add coherently, despite that fact that they rotate with the same phase velocity, because the stationary phases, $\varphi_0^{1,n+j}$, are *randomly* distributed. On the locked branch of solutions, the above expression simplifies to

$$\psi(r,\theta,\phi,t) = \left(\sum_{j=0}^{N-1} A_{n+j}(r) e^{-ij\varphi_*}\right) e^{i(\theta - n\phi + \varphi_0^{1,n} + n\Omega_* t)}, \tag{102}$$

where $\varphi_*(\phi,t)$ is defined in Eq. (63), and use has been made of Eqs. (99) and (100). Here, it is assumed that the $1,n$ through $1,n+N-1$ tearing modes are strongly locked. By analogy with the discussion in Sec. II F, it is clear that the correlation in the stationary phases of the $m = 1$ tearing modes associated with locking [see Eq. (99)] gives rise to the development of a toroidally localized, coherent, interference pattern in the perturbed magnetic field that corotates with the plasma at the reversal surface. As before, the toroidal angular width of this pattern, which is approximately $4\pi/N$, is determined solely by the number of locked $m = 1$ modes. However, unlike the previous case, there are no high-frequency, high-n oscillations contained within the interference pattern, since the constituent $m = 1$ modes all rotate toroidally with the same phase velocity as the pattern itself. Of course, this toroidally localized interference pattern is again identified with the "slinky mode." Note that, in the presence of enhanced core viscosity, the observation of a slowly rotating slinky mode *does* necessarily imply that the plasma core is slowly rotating.

5. Discussion

The above analysis demonstrates that enhanced core viscosity significantly modifies the locking process by forcing the saturated $m = 1$ tearing modes in the plasma core to always rotate with identical phase velocities. This, in turn, forces the plasma core to corotate with the plasma at the reversal surface after locking has occurred. Thus, in general, there is a significant reduction in the core toroidal rotation after locking. On the other hand, in the absence of enhanced core viscosity, the locking bifurcation is only associated with a slight redistribution in the plasma toroidal angular momentum interior to the reversal surface. In this case, there is no significant reduction in the core rotation after locking. The core viscosity also affects the nature of the slinky mode. In

the absence of enhanced core viscosity, the slinky mode forms a toroidally localized, slowly rotating envelope within which high-frequency, high-n oscillations, controlled by the core plasma rotation, take place. However, there are no such oscillations in the presence of enhanced core viscosity.

A careful examination of Eqs. (25)–(27), (74), and (75) demonstrates that the core viscosity can only be regarded as being enhanced, provided that

$$\mu_n \gg n\mu_* , \qquad (103)$$

where μ_n is the typical core viscosity, μ_* is the typical viscosity at the reversal surface, and n is the typical toroidal mode number of a saturated $m=1$ tearing mode. Conversely, the core viscosity cannot be regarded as being enhanced whenever

$$\mu_n \ll n\mu_* . \qquad (104)$$

As an added complication, since the core viscosity is largely generated by magnetic stochasticity associated with the saturated $m=1$ tearing modes in the plasma core, the level of enhancement is almost certainly a *strongly increasing* function of the amplitudes of these modes. Thus, the enhancement level may change systematically during a sawtooth relaxation cycle. It may also differ significantly from machine to machine, and also between different modes of operation on the same machine.

Incidentally, in the presence of enhanced core viscosity it is not necessary to invoke strong poloidal flow damping to justify the neglect of the poloidal torques. Since these torques are only capable of modifying the plasma rotation *interior* to the core (i.e., for $r < r_{n+N-1}$), they are naturally rendered ineffective by enhanced core viscosity.

III. LOCKING OF THE SLINKY MODE

A. Introduction

Consider the locking of the slinky mode to a static error field, a process by which the mode rotation is *arrested* in the laboratory frame. Since the rotation of the slinky mode is entirely determined by the plasma rotation velocity at the reversal surface (see Sec. II), it is natural to concentrate on the effect of a 0,1 error field, which is resonant at this surface. There are two possibilities. Either the error field arrests the rotation of the plasma at the reversal surface *before* the formation of the slinky mode, so that the mode subsequently forms as a *locked* (i.e., nonrotating) mode, or the slinky mode forms as a *rotating* mode that subsequently locks to the error field. In the following, these two possibilities are considered separately.

B. Locking of the reversal surface to a static error field

1. Basic equations

The dispersion relation for the 0,1 mode in the presence of a 0,1 error field, but in the absence of a slinky mode, takes the form [see Appendix B and Eq. (11)]

$$\Delta^{0,1}(\omega_*)\Psi^{0,1} \equiv \Delta\Psi^{0,1} = E^{0,1}\Psi^{0,1} + C^{0,1}. \qquad (105)$$

Here, the complex quantity $\Delta^{0,1}$ is the layer response function for the 0,1 mode (see Appendix A 5), ω_* is the frequency of the static error field, as seen in a frame of reference that corotates with the plasma at the reversal surface, the real quantity $E^{0,1}$ (n.b., $E^{0,1}<0$) is the tearing stability index for the 0,1 mode (see Appendix A 3), and the complex quantity $C^{0,1}$ specifies the amplitude and phase of the 0,1 error field at the reversal surface (see Appendix B). It follows that

$$\omega_* = \Omega_* , \qquad (106)$$

where Ω_* is the plasma toroidal angular velocity at the reversal surface.

The toroidal electromagnetic torque exerted at the reversal surface by the error field is written [see Eq. (B6)]

$$\delta T^{0,1}_{\phi\,\text{EM}} = \frac{2\pi^2 R_0}{\mu_0} \frac{\text{Im}[C^{0,1}(\Psi^{0,1})^*]}{H^{0,1}(r_*)} . \qquad (107)$$

Balancing this torque against the viscous restoring torque that develops at the reversal surface (calculated according to the prescription of Sec. II C), yields the torque balance equation,

$$\omega_* - \omega_*^{(0)} = L_* \tilde{T}_*(\omega_*), \qquad (108)$$

where

$$L_* = \int_{r_*}^{a} \frac{\mu_*}{\mu} \frac{dr}{r}, \qquad (109)$$

and $\tilde{T}_* = \delta T^{0,1}_{\phi\,\text{EM}}/(4\pi^2 R_0^3 \mu_*)$. Note that $\omega_*^{(0)}$ is the value of ω_* in the unperturbed plasma. It follows that

$$\omega_*^{(0)} = \Omega_*^{(0)}, \qquad (110)$$

where $\Omega_*^{(0)}$ is the value of the toroidal angular velocity of the plasma at the reversal surface in the unperturbed state. The plasma angular velocity inside the reversal surface is simply given by

$$\Omega(r<r_*) = \Omega^{(0)}(r<r_*) + \Omega_* - \Omega_*^{(0)} . \qquad (111)$$

Note that none of the nonlinear frequencies, ω_{n+j}, defined in Eq. (12), are affected by the modification to the plasma toroidal rotation profile induced by a 0,1 error field.

2. Linear analysis

It follows from Eqs. (105) and (107) that

$$\tilde{T}_* = \frac{1}{2} \frac{\tau_V}{\tau_H^2} (\tilde{C}^{0,1})^2 \frac{\text{Im}[\Delta^{0,1}(\omega_*)]}{|\Delta^{0,1}(\omega_*) - E^{0,1}|^2}, \qquad (112)$$

where τ_H and τ_V are defined in Eqs. (29) and (30), respectively, and

$$\tilde{C}^{0,1} = \frac{|C^{0,1}|}{r_*^2 F_*'} . \qquad (113)$$

Here, F_*' is defined in Eq. (34).

Using the explicit form (37) for the layer response function, the torque balance equation (108) can be written as

$$\frac{1}{4}\frac{(\widetilde{C}^{0,1})^2}{\Lambda_*^2}\frac{\hat{\omega}_*}{\zeta_*^2+\hat{\omega}_*^2}=1-\hat{\omega}_*, \tag{114}$$

where use has been made of Eq. (112), and

$$\hat{\omega}_*=\frac{\omega_*}{\omega_*^{(0)}}, \tag{115}$$

$$\zeta_*=\frac{-E^{0,1}}{\omega_*^{(0)}\tau_*}, \tag{116}$$

$$\Lambda_*^2=\frac{1}{2}\left.\frac{[\omega_*^{(0)}]^2\tau_*\tau_H^2}{\tau_V}\right/L_*. \tag{117}$$

Here, τ_* is defined in Eq. (38).

Equation (114) is, of course, the standard induction motor equation [see Eq. (40)]. In the physically relevant limit $\zeta_*\ll1$, there are two branches of solutions (see the discussion in Sec. II E). On the *unlocked* branch, there is substantial plasma rotation at the reversal surface, which effectively suppresses any error-field driven magnetic reconnection, whereas on the *locked* branch the plasma rotation at the reversal surface is arrested, and a nonrotating, error-field driven, magnetic island chain forms. The unlocked branch of solutions ceases to exist for

$$\widetilde{C}^{0,1}\geqslant\Lambda_*. \tag{118}$$

A *locking* bifurcation (i.e., a bifurcation from the unlocked to the locked branches) takes place when the error-field amplitude (i.e., $\widetilde{C}^{0,1}$) exceeds the critical value given above. Likewise, the locked branch of solutions ceases to exist for

$$\widetilde{C}^{0,1}\leqslant(8\zeta_*)^{1/2}\Lambda_*. \tag{119}$$

An *unlocking* bifurcation (i.e., a bifurcation from the locked to the unlocked branches) takes place when the error-field amplitude falls below the critical value given above. As always, there is considerable *hysteresis* in the locking process, since the critical error-field amplitude for locking [given in Eq. (118)] is much greater than that for unlocking [given in Eq. (119)].

3. Nonlinear analysis

On the locked branch of solutions, the *no-slip* constraint (see the discussion in Sec. II E) demands that

$$\omega_*=0. \tag{120}$$

In other words, the plasma rotation at the reversal surface is completely arrested after locking.

According to Eq. (B27), $C^{0,1}$ can be written as

$$C^{0,1}=c^{0,1}\Psi_{\text{gap}}^{0,1}, \tag{121}$$

where $c^{0,1}$ is a real positive parameter, specified by Eq. (B28), and $\Psi_{\text{gap}}^{0,1}$ is a complex parameter that determines the amplitude and phase of the 0,1 error field leaking through the gaps in the conducting shell. Let

$$\Psi_{\text{gap}}^{0,1}=\hat{\Psi}_{gap}^{0,1}e^{i\varphi_{\text{gap}}^{0,1}}, \tag{122}$$

where $\hat{\Psi}_{\text{gap}}^{0,1}\equiv|\Psi_{\text{gap}}^{0,1}|$, and $\varphi_{\text{gap}}^{0,1}\equiv\arg(\Psi_{\text{gap}}^{0,1})$.

On the locked branch of solutions, the 0,1 reconnected flux driven by the error field at the reversal surface is determined by the Rutherford island equation (A37), which yields

$$4I\tau_R\frac{d(\sqrt{\widetilde{\Psi}^{0,1}})}{dt}=\text{Re}\left(\frac{\Delta\Psi^{0,1}}{\Psi^{0,1}}\right)=E^{0,1}+\frac{\widetilde{C}^{0,1}}{\widetilde{\Psi}^{0,1}}\cos\Delta\varphi_*, \tag{123}$$

where $I=0.8227$, $\widetilde{\Psi}^{0,1}=\hat{\Psi}^{0,1}/r_*^2F_*'$, and τ_R is defined in Eq. (39). Here,

$$\Delta\varphi_*=\varphi_0^{0,1}-\varphi_{\text{gap}}^{0,1}, \tag{124}$$

and use has been made of Eqs. (3), (4), (106), and (120)–(122).

The torque balance equation (108) reduces to

$$\omega_*^{(0)}=\frac{L_*}{2}\frac{\tau_V}{\tau_H^2}\widetilde{C}^{0,1}\widetilde{\Psi}^{0,1}\sin\Delta\varphi_*, \tag{125}$$

on the locked branch of solutions.

In steady state, Eqs. (123) and (125) yield

$$8\zeta_*\Lambda_*^2=(\widetilde{C}^{0,1})^2\sin2\Delta\varphi_*. \tag{126}$$

Note that the locked branch of solutions ceases to exist for

$$\widetilde{C}^{0,1}\leqslant(8\zeta_*)^{1/2}\Lambda_*. \tag{127}$$

When the error-field amplitude, $\widetilde{C}^{0,1}$, falls below this critical value, an unlocking bifurcation takes place.

The unlocking threshold (127) predicted by nonlinear theory is the same as the threshold (119) predicted by linear theory. However, as discussed in Sec. II E, this is somewhat fortuitous. In general, the correct unlocking threshold is that predicted by nonlinear theory. On the other hand, the locking threshold (118) predicted by linear theory is generally correct.

In the strongly locked limit, in which the error-field amplitude lies well above the unlocking threshold, Eq. (126) yields

$$\Delta\varphi_*\simeq0. \tag{128}$$

C. Formation of a locked slinky mode

1. Basic equations

Consider the formation of a slinky mode when the reversal surface is strongly locked to a static error field (i.e., when $\omega_*=\Delta\varphi_*=0$). The presence of an error-field-driven, locked magnetic island chain at the reversal surface precludes the use of linear response theory. However, the Rutherford island equation yields

$$4I\tau_R\frac{d\sqrt{\widetilde{\Psi}^{0,1}}}{dt}$$

$$=E^{0,1}+\left(\sum_{j=0}^{N-2}\chi_{n+j}\cos(\omega_{n+j}t)+\widetilde{C}^{0,1}\right)\bigg/\widetilde{\Psi}^{0,1}. \tag{129}$$

Furthermore, the nonlinear electromagnetic torques exerted inside the plasma can be written as

$$\tilde{T}_{n+j} = \frac{1}{2} \frac{\tau_V}{\tau_H^2} \chi_{n+j} \tilde{\Psi}^{0,1} \sin(\omega_{n+j} t), \qquad (130)$$

for $j = 0, N-2$, where use has been made of Eqs. (8) and (9).

2. Slinky mode formation

Let

$$\tilde{\Psi}^{0,1}(t) = \tilde{\Psi}_{(0)}^{0,1} + \tilde{\Psi}_{(1)}^{0,1}(t), \qquad (131)$$

where

$$\tilde{\Psi}_{(0)}^{0,1} = \frac{\tilde{C}^{0,1}}{-E^{0,1}} \qquad (132)$$

and

$$|\tilde{\Psi}_{(1)}^{0,1}| \ll \tilde{\Psi}_{(0)}^{0,1}. \qquad (133)$$

It follows from Eq. (129) that

$$\frac{W_C}{r_*} \frac{\tau_R}{2} \frac{d\tilde{\Psi}_{(1)}^{0,1}}{dt} \simeq \sum_{j=0}^{N-2} \chi_{n+j} \cos(\omega_{n+j} t), \qquad (134)$$

where

$$W_C = 4 \sqrt{\tilde{\Psi}_{(0)}^{0,1}} r_* = 4 \sqrt{\frac{\tilde{C}^{0,1}}{-E^{0,1}}} r_* \qquad (135)$$

is the width of the error-field-driven island chain at the reversal surface.

Equation (134) yields

$$\tilde{\Psi}_{(1)}^{0,1} \simeq \frac{2 \sum_{j=0}^{N-2} \chi_{n+j} \sin(\omega_{n+j} t)}{I(W_C/r_*) \tau_R \omega_{n+j}}. \qquad (136)$$

Thus,

$$\tilde{T}_{n+j} = \frac{1}{2} \frac{\tau_V}{\tau_H^2} \chi_{n+j} \left(\tilde{\Psi}_{(0)}^{0,1} + \frac{2 \sum_{k=0}^{N-2} \chi_{n+k} \sin(\omega_{n+k} t)}{I(W_C/r_*) \tau_R \omega_{n+k}} \right)$$
$$\times \sin(\omega_{n+j} t). \qquad (137)$$

Note that the nonlinear electromagnetic torques $\tilde{T}_{n+j}$ *oscillate* in time. In this paper, however, it is assumed that the plasma is sufficiently viscous that it only responds to the *steady* components of these torques, which is equivalent to the assumption that the plasma continues to rotate *uniformly* in the presence of the oscillating nonlinear torques (i.e., the frequencies ω_{n+j} remain constant in time). This approximation, which is discussed in more detail in Refs. 11 and 13, is justified, provided that

$$\sqrt{\omega_{n+j}^{(0)} \tau_V} \gg 1, \qquad (138)$$

for $j = 0, N-2$, as is likely to be the case in all conventional RFP plasmas.

According to the above discussion, the nonlinear torque $\tilde{T}_{n+j}$ can effectively be replaced by its time-averaged value: i.e.,

$$\tilde{T}_{n+j} \to \langle \tilde{T}_{n+j} \rangle = \frac{1}{2} \frac{\tau_V}{\tau_H^2} \frac{\chi_{n+j}^2}{I(W_C/\tau_*) \tau_R \omega_{n+j}}. \qquad (139)$$

Now, from linear response theory, the nonlinear torques on the unlocked branch of solutions can be written as

$$\bar{T}_{n+j} = \frac{1}{2} \frac{\tau_V}{\tau_H^2} \frac{\chi_{n+j}^2}{\tau_* \omega_{n+j}}, \qquad (140)$$

where

$$\tau_* = \frac{\delta_*}{\tau_*} \tau_R. \qquad (141)$$

Here, use has been made of Eqs. (28), (37), and (38). Furthermore,

$$\delta_* = 2.104 \frac{\tau_H^{1/3}}{\tau_V^{1/6} \tau_R^{1/6}} r_* \qquad (142)$$

is the linear layer width at the reversal surface [see Eq. (A40)]. It is clear, from a comparison of Eqs. (139) and (140), that the only difference between linear and nonlinear response theory, at the reversal surface, is that the linear layer width δ_* is replaced by the modified island width IW_C in the latter case.

The above insight allows Eq. (67), which govern the formation of the slinky mode, to be generalized in a fairly straightforward manner to give

$$1 - \hat{\omega}_{n+j} = \frac{1}{4g_*} \left(\sum_{k=0}^{j-1} \lambda_{n+k,n+j} \frac{\chi_{n+k}^2}{\Lambda_{n+k}^2 \hat{\omega}_{n+k}} + \frac{\chi_{n+j}^2}{\Lambda_{n+j}^2 \hat{\omega}_{n+j}} + \sum_{k=j+1}^{N-2} \kappa_{n+j,n+k} \frac{\chi_{n+k}^2}{\Lambda_{n+k}^2 \hat{\omega}_{n+k}} \right), \qquad (143)$$

for $j = 0, N-2$. Here,

$$g_* = \begin{cases} 1, & \text{for } \delta_* > IW_C, \\ IW_C/\delta_*, & \text{for } \delta_* < IW_C. \end{cases} \qquad (144)$$

Note that, in general, the formation of the slinky mode is somewhat inhibited when the reversal surface is locked to a static error field (i.e., the mode amplitudes χ_{n+j} must be made slightly larger in order to trigger slinky mode formation).

For the special case of enhanced core viscosity, the slinky formation criterion (95) generalizes to

$$\sum_{j=0}^{N-2} \chi_{n+j}^2 \gtrsim g_* \Lambda_c^2. \qquad (145)$$

3. Slinky mode breakup

Equation (72), which govern the breakup of the slinky mode, generalize in a fairly obvious manner when the reversal surface is strongly locked to a static error field to give

$$1 = \frac{1}{4} \left(\sum_{j=0}^{N-2} \chi_{n+j} \cos \Delta \varphi_{n+j} + \tilde{C}^{0,1} \right)$$
$$\times \left(\sum_{k=0}^{j-1} \lambda_{n+k,n+j} \frac{\chi_{n+k}}{\zeta_{n+k} \Lambda_{n+k}^2} \sin \Delta \varphi_{n+k} \right.$$
$$+ \frac{\chi_{n+j}}{\zeta_{n+j} \Lambda_{n+j}^2} \sin \Delta \varphi_{n+j}$$

$$+ \sum_{k=j+1}^{N-2} \kappa_{n+j,n+k} \frac{\chi_{n+k}}{\zeta_{n+k}\Lambda_{n+k}^2} \sin \Delta\varphi_{n+k} \Bigg), \qquad (146)$$

for $j=0, N-2$.

For the special case of enhanced core viscosity, the above expression reduces to

$$4\zeta_n\Lambda_c^2 = \Bigg[\left(\sum_{j=0}^{N-2} \chi_{n+j} \right) \cos \Delta\varphi_n + \tilde{C}^{0,1} \Bigg]$$
$$\times \left(\sum_{j=0}^{N-2} \chi_{n+j} \right) \sin \Delta\varphi_n. \qquad (147)$$

As is easily demonstrated, the criterion for the breakup of the slinky mode is written as

$$\left(\sum_{j=0}^{N-2} \chi_{n+j} \right)^2 \leq 8\zeta_n\Lambda_c^2, \qquad (148)$$

in the limit $\tilde{C}^{0,1} \ll \Sigma_{j=0}^{N-2}\chi_{n+j}$, which is the same as the breakup criterion found previously [see Eq. (98)]. However, in the limit $\tilde{C}^{0,1} \gg \Sigma_{j=0}^{N-2}\chi_{n+j}$ the breakup criterion becomes

$$\tilde{C}^{0,1} \left(\sum_{j=0}^{N-2} \chi_{n+j} \right) \leq 4\zeta_n\Lambda_c^2. \qquad (149)$$

Note that, in general, the breakup of the slinky mode is somewhat inhibited when the reversal surface is locked to a static error field (i.e., the mode amplitudes χ_{n+j} must be made slightly smaller in order to trigger slinky mode breakup).

D. Locking of a slinky mode to a static error field

1. Basic equations

Consider the interaction of a rotating slinky mode whose constituent $m=1$ modes are strongly locked together (i.e., $\omega_{n+j} = \Delta\varphi_{n+j} = 0$, for $j=0, N-2$) with a static 0,1 error field that is not sufficiently strong to arrest the plasma rotation at the reversal surface in the absence of a slinky mode. It follows that $\omega_* \neq 0$ (initially). The presence of a nonlinearly driven, rotating magnetic island chain at the reversal surface precludes the use of linear response theory. However, the Rutherford island equation yields

$$4I\tau_R \frac{d\sqrt{\tilde{\Psi}^{0,1}}}{dt}$$
$$= E^{0,1} + \left(\sum_{j=0}^{N-2} \chi_{n+j} + \tilde{C}^{0,1}\cos(\omega_* t) \right) \Big/ \sqrt{\tilde{\Psi}^{0,1}}. \qquad (150)$$

Furthermore, the toroidal electromagnetic torque exerted at the reversal surface is written as

$$\tilde{T}_* = -\frac{1}{2}\frac{\tau_V}{\tau_H^2}\tilde{C}^{0,1}\sqrt{\tilde{\Psi}^{0,1}}\sin(\omega_* t). \qquad (151)$$

The frequency ω_*, which parametrizes the plasma rotation at the reversal surface, is determined by the torque balance equation (108).

2. Mode locking

Let

$$\sqrt{\tilde{\Psi}^{0,1}}(t) = \sqrt{\tilde{\Psi}_{(0)}^{0,1}} + \tilde{\Psi}_{(1)}^{0,1}(t), \qquad (152)$$

where

$$\sqrt{\tilde{\Psi}_{(0)}^{0,1}} = \frac{\Sigma_{j=0}^{N-2}\chi_{n+j}}{-E^{0,1}}, \qquad (153)$$

and

$$|\tilde{\Psi}_{(1)}^{0,1}| \ll \sqrt{\tilde{\Psi}_{(0)}^{0,1}}. \qquad (154)$$

It follows from Eq. (150) that

$$\frac{W_\chi}{r_*}\frac{\tau_R}{2}\frac{d\tilde{\Psi}_{(1)}^{0,1}}{dt} \simeq \tilde{C}^{0,1}\cos(\omega_* t), \qquad (155)$$

where

$$W_\chi = 4\sqrt{\sqrt{\tilde{\Psi}_{(0)}^{0,1}}}r_* = 4\sqrt{\frac{\Sigma_{j=0}^{N-2}\chi_{n+j}}{-E^{0,1}}}r_* \qquad (156)$$

is the width of the nonlinearly driven island chain at the reversal surface.

Equation (155) yields

$$\tilde{\Psi}_{(1)}^{0,1} \simeq \frac{2\tilde{C}^{0,1}\sin(\omega_* t)}{I(W_\chi/r_*)\tau_R\omega_*}. \qquad (157)$$

Thus,

$$\tilde{T}_* = -\frac{1}{2}\frac{\tau_V}{\tau_H^2}\tilde{C}^{0,1}\Bigg[\sqrt{\tilde{\Psi}_{(0)}^{0,1}} + \frac{2\tilde{C}^{0,1}\sin(\omega_* t)}{I(W_\chi/r_*)\tau_R\omega_{n+k}} \Bigg]\sin(\omega_* t). \qquad (158)$$

Note that the locking torque $\tilde{T}_*$ *oscillates* in time. As before, it is assumed that the plasma is sufficiently viscous that it only responds to the *steady* component of this torque. This approximation is justified, provided that[13]

$$\sqrt{\omega_*^{(0)}\tau_V} \gg 1, \qquad (159)$$

as is likely to be the case in all conventional RFP plasmas.

According to the above discussion, the locking torque $\tilde{T}_*$ can effectively be replaced by its time-averaged value: i.e.,

$$\tilde{T}_* \to \langle\tilde{T}_*\rangle = -\frac{1}{2}\frac{\tau_V}{\tau_H^2}\frac{(\tilde{C}^{0,1})^2}{I(W_\chi/r_*)\tau_R\omega_*}. \qquad (160)$$

Hence, the torque balance equation (108) reduces to

$$\hat{\omega}_*(1-\hat{\omega}_*) = \frac{(\tilde{C}^{0,1})^2}{4\Lambda_*^2(IW_\chi/\delta_*)}. \qquad (161)$$

It is easily seen, from the above expression, that the un-locked branch of solutions ceases to exist for

$$\tilde{C}^{0,1} \geq \sqrt{IW_\chi/\delta_*}\Lambda_*. \qquad (162)$$

When the error-field amplitude (i.e., $\tilde{C}^{0,1}$) exceeds the critical value given above a locking bifurcation (i.e., a bifurcation from the unlocked to the locked branch of solutions)

takes place. Of course, on the locked branch of solutions both the plasma rotation at the reversal surface and the rotation of the slinky mode are arrested.

Note that the locking criterion given in Eq. (162) is similar to that found previously in Eq. (118), except that the linear layer width δ_* is replaced by the modified island width IW_χ in the former case. The generalized locking criterion, which accounts for the locking of the reversal surface by a 0, 1 error field both in the absence and in the presence of a rotating slinky mode, is written as

$$\widetilde{C}^{0,1} \geqslant \sqrt{g_\chi} \Lambda_*, \tag{163}$$

where

$$g_\chi = \begin{cases} 1, & \text{for } \delta_* > IW_\chi, \\ IW_\chi/\delta_*, & \text{for } \delta_* < IW_\chi. \end{cases} \tag{164}$$

Note that, in general, the locking of the reversal surface is somewhat inhibited in the presence of a rotating slinky mode (i.e., the error-field amplitude $\widetilde{C}^{0,1}$ must be made slightly larger in order to trigger locking).

3. Mode unlocking

On the locked branch of solutions, where $\omega_* = 0$, the Rutherford island equation reduces to

$$4I\tau_R \frac{d\sqrt{\widetilde{\Psi}^{0,1}}}{dt}$$
$$= E^{0,1} + \left(\sum_{j=0}^{N-2} \chi_{n+j} + \widetilde{C}^{0,1} \cos \Delta\varphi_* \right) \bigg/ \sqrt{\widetilde{\Psi}^{0,1}}. \tag{165}$$

Furthermore, the torque balance equation takes the form given in Eq. (125). In steady state, these equations yield

$$4\zeta_* \Lambda_*^2 = \left(\sum_{j=0}^{N-2} \chi_{n+j} + \widetilde{C}^{0,1} \cos \Delta\varphi_* \right) \widetilde{C}^{0,1} \sin \Delta\varphi_*. \tag{166}$$

As is easily demonstrated, the criterion for the unlocking of the slinky mode is written

$$(\widetilde{C}^{0,1})^2 \leqslant 8\zeta_* \Lambda_*^2, \tag{167}$$

in the limit $\Sigma_{j=0}^{N-2} \chi_{n+j} \ll \widetilde{C}^{0,1}$, which is the same as the criterion found previously [see Eq. (127)]. However, in the limit $\Sigma_{j=0}^{N-2} \chi_{n+j} \gg \widetilde{C}^{0,1}$ the unlocking criterion becomes

$$\widetilde{C}^{0,1} \left(\sum_{j=0}^{N-2} \chi_{n+j} \right) \leqslant 4\zeta_* \Lambda_*^2. \tag{168}$$

Note that, in general, the unlocking of the reversal surface is somewhat inhibited in the presence of a locked slinky mode (i.e., the error-field amplitude $\widetilde{C}^{0,1}$ must be made slightly smaller in order to trigger unlocking).

E. The toroidal locking angle

Consider a slinky mode whose constituent $m=1$ modes are strongly locked together (i.e., $\omega_{n+j} = \Delta\varphi_{n+j} = 0$, for $j = 0, N-2$). Suppose that the mode is, in turn, strongly locked to a 0, 1 error field (i.e., $\omega_* = \Omega_* = \Delta\varphi_* = 0$). Recall,

from Sec. II F, that the magnetic perturbation associated with a slinky mode is strongly peaked at the toroidal angle,

$$\phi_{\text{lock}} = \varphi_0^{0,1}, \tag{169}$$

obtained from setting φ_* to zero—see Eq. (63). However, it follows from Eq. (124) that

$$\phi_{\text{lock}} = \varphi_{\text{gap}}^{0,1}, \tag{170}$$

since $\Delta\varphi_* = 0$ for a strongly locked mode, where $\varphi_{\text{gap}}^{0,1}$ is defined in Eq. (122).

The dominant error-field source in a RFP is usually a 1,0 field arising from the mismatch between the ''vertical'' magnetic fields interior and exterior to the shell. Of course, the plasma experiences this field filtered through the gaps in the shell. Suppose that the mismatched ''vertical'' field is of magnitude B_v, and is directed toward poloidal angle θ_v. In this paper, $\theta=0$ corresponds to the *inboard midplane*. Thus, $\theta_v = \pm\pi/2$ corresponds to a true vertical field, whereas $\theta_v = 0, \pi$ corresponds to a horizontal field.

Suppose, for example, that the flux-conserving shell contains two vacuum gaps: a *poloidal* gap, extending from $\phi = \phi_g - \Delta\phi/2$ to $\phi = \phi_g + \Delta\phi/2$, and a *toroidal* gap, extending from $\theta = \theta_g - \Delta\theta/2$ to $\theta = \theta_g + \Delta\theta/2$. The gaps are both assumed to be *thin*: i.e., $\Delta\phi, \Delta\theta \ll \pi$. It follows from Eqs. (122), (170), and (B31) that

$$\phi_{\text{lock}} = \varphi_{\text{gap}}^{0,1} = \phi_g + (\theta_g - \theta_v), \tag{171}$$

in this case. Thus, the slinky mode only locks to the poloidal gap (i.e., $\phi_{\text{lock}} = \phi_g$) when the ''vertical'' error field points toward the toroidal gap (i.e., when $\theta_v = \theta_g$). If there is a mismatch between the direction of the ''vertical'' error field and the poloidal location of the toroidal gap, then there is a corresponding mismatch between the locking angle of the slinky mode and the toroidal location of the poloidal gap.

F. Locked mode alleviation

Slinky modes are generally associated with a significant increase in the plasma radial heat transport. Naturally, this confinement degradation tends to be strongly peaked at the toroidal localization angle of the perturbed magnetic field. Thus, a slinky mode gives rise to a toroidally localized anomalous heat flux out of the plasma, whose toroidal position corotates with the mode. This heat flux is not generally problematic, as long as the slinky mode remains rotating, since the heat load is spread over a relatively large area of the plasma facing surface. However, if the mode locks to an error field, and, thereby, ceases to rotate, the heat load becomes concentrated on a relatively small area, which, almost invariably, leads to overheating, the influx of impurities into the plasma, and the premature termination of the discharge.[9]

There are two obvious methods by which the problems associated with a locked slinky mode can be alleviated. The first method is to cancel out the error field that is responsible for the locking, using a second, deliberately created, *static* error field, thereby allowing the slinky mode to unlock, and, hence, rotate (rapidly). The second method is to (slowly)

rotate the locking position of the slinky mode using a deliberately created, *rotating* error field.[29] These two approaches are considered separately below.

The accidentally produced error field that is responsible for locking the slinky mode is assumed to be a 1, 0 ''vertical'' field of the type discussed in Sec. III E. Suppose that the second, deliberately produced error field, which is used to alleviate the locking problems, is a 0, 1 perturbation. This is a natural choice, since it is the 0, 1 component of the error field that is responsible for the locking problems in the first place. In vacuum, the radial component of the second ''control'' field, at the shell radius b, is assumed to attain its maximum amplitude B_c at toroidal angle ϕ_c. Of course, the plasma experiences both error fields filtered through the gaps in the conducting shell. It follows from Appendix B 6 that

$$\Psi_{gap}^{0,1} = bf[B_v e^{i\phi_{lock}} + B_c e^{i\phi_c}], \qquad (172)$$

where f is the area fraction of gaps in the conducting shell. According to Eq. (121), the normalized amplitude of the 0,1 error field at the reversal surface can be written as

$$\widetilde{C}^{0,1} = c^{0,1}f[\widetilde{B}_v^2 + \widetilde{B}_c^2 + 2\widetilde{B}_v\widetilde{B}_c \cos(\phi_c - \phi_{lock})]^{1/2}, \quad (173)$$

where $\widetilde{B}_v = bB_v/r_*^2 F_*'$ and $\widetilde{B}_c = bB_c/r_*^2 F_*'$. Here, $\widetilde{B}_v$ and $\widetilde{B}_c$ are dimensionless quantities parametrizing the magnitudes of the ''vertical'' mismatch field and the control field, respectively, whereas $c^{0,1}$ is a real positive constant defined in Eq. (B28). The amplitude of the 0,1 error field is most effectively minimized when the control field is in *antiphase* with the original locking phase of the slinky mode: i.e., when

$$\phi_c = \phi_{lock} + \pi. \qquad (174)$$

In this case,

$$\widetilde{C}^{0,1} = c^{0,1}f|\widetilde{B}_v - \widetilde{B}_c|. \qquad (175)$$

Note that $\widetilde{C}^{0,1} \to 0$ as $B_c \to B_v$. If $\widetilde{C}^{0,1}$ is made sufficiently small then the slinky mode will either unlock, and start to rotate, or breakup altogether, depending on which threshold is reached first. The unlocking threshold is specified in Eqs. (167) and (168), whereas the breakup threshold is determined by Eq. (146).

The thick conducting shell that surrounds a conventional RFP generally makes it difficult to control the plasma vertical and horizontal positions. Consequently, the 1,0 ''vertical'' mismatch field at the gaps in the shell tends to be relatively large, and also *fluctuates* in time. Thus, it may not be practical to cancel out the 0,1 component of this field, which also fluctuates in time. An alternative, and more practical, locked mode alleviation scheme is to use a rotating 0,1 error field to *sweep* the locking angle of the slinky mode, thereby reducing the heat load associated with this mode on the plasma facing surface. This approach has already been successfully implemented on the RFX device.[29] Suppose that the control field rotates uniformly at some relatively low-frequency ω_c: i.e.,

$$\phi_c = \omega_c t. \qquad (176)$$

It follows from Eqs. (122), (170), and (172) that the deviation of the slinky mode locking angle from its unperturbed value satisfies

$$\tan \Delta\varphi_{lock} = \frac{(B_c/B_v)\sin \omega_c t}{1 + (B_c/B_v)\cos \omega_c t}. \qquad (177)$$

For $B_c < B_v$, the locking angle oscillates about its unperturbed value. The amplitude of the oscillation is given by

$$(\Delta\varphi_{lock})_{max} = \sin^{-1}(B_c/B_v). \qquad (178)$$

However, for $B_c > B_v$ the locking angle executes complete toroidal rotations around the device with angular frequency ω_c.

IV. SUMMARY

In Sec. II of this paper we examine the formation of the slinky mode via the nonlinear coupling of multiple $m = 1$ tearing modes resonant in the plasma core. This coupling is mediated by the nonlinearly driven 0, 1 mode, resonant at the reversal surface. The slinky mode forms as a result of a locking bifurcation. Likewise, the slinky mode breaks up as the result of an unlocking bifurcation. However, there is considerable hysteresis in the formation and breakup processes, since the locking threshold [which is obtained from Eq. (67)] is much smaller than the unlocking threshold [which is obtained from Eq. (72)], when both are expressed in terms of the typical amplitude of an $m = 1$ tearing mode in the plasma core.

In general, the locking bifurcation by which a slinky mode forms is associated with a *slight* redistribution of the plasma toroidal angular momentum in the plasma core. This redistribution modifies the rotation frequencies of the core tearing modes such that they add *coherently* at one particular toroidal angle [see Sec. II F 4]. This angle [which is specific by $\varphi_* = 0$—see Eq. (63)] rotates toroidally with the angular velocity of the plasma at the reversal surface. Thus, the slinky mode takes the form of a toroidally localized, coherent interference pattern in the magnetic field that corotates with the plasma at the reversal surface. The toroidal angular width of this pattern is determined solely by the number of locked $m = 1$ modes. The larger the number of modes, the narrow the width of the pattern. In general, the slinky mode constitutes a relatively slowly rotating envelope within which the magnetic field exhibits high-n, high-frequency oscillations (assuming, as seems reasonable, that the plasma core rotates far more rapidly than the plasma at the reversal surface). The nature of these high-frequency oscillations is determined by the core plasma rotation rate, as well as the toroidal mode numbers of the $m = 1$ modes that make up the slinky pattern. Note that, in general, the occurrence of a slowly rotating slinky mode *does not* necessarily imply that the plasma core is slowly rotating.

In Sec. II G we examine the effect of an enhanced (perpendicular) plasma viscosity in the plasma core, relative to that at the plasma edge, on the formation and breakup of the slinky mode. Such an enhancement is likely to develop naturally in a RFP due to the stochasticity of the core magnetic field generated by overlapping magnetic islands. An en-

hanced core viscosity significantly modifies the slinky formation process by forcing the saturated $m = 1$ tearing modes in the plasma core to always rotate with identical phase velocities. This, in turn, requires the plasma core to corotate with the plasma at the reversal surface after the formation of the slinky mode. It follows that, in the presence of enhanced core viscosity, the formation of the slinky mode is associated with a significant reduction in the core plasma rotation. Enhanced core viscosity greatly simplifies the locking and unlocking bifurcations by which the slinky mode forms and breaks up, respectively, since it forces all of the $m = 1$ tearing modes in the plasma core to lock and unlock *simultaneously*. In the absence of enhanced core viscosity, the slinky mode generally forms and breaks up in a piecemeal manner. Consequently, in the presence of enhanced core viscosity, the slinky formation and breakup thresholds take the particularly simple forms (95) and (98), respectively. An enhanced core viscosity also modifies the structure of the slinky mode by suppressing the high-n, high-frequency oscillations described previously. The criterion that must be satisfied before the core plasma viscosity can be regarded as being enhanced is given in Eq. (103).

In Sec. III of this paper we examine the interaction of a slinky mode with a static error field. This interaction is mediated by the 0,1 component of the field, which is resonant at the reversal surface. Either the error field arrests the rotation of the plasma at the reversal surface before the formation of the slinky mode (see Sec. III B), so that the mode subsequently forms as a nonrotating mode (see Sec. III C), or the slinky mode forms as a rotating mode and subsequently locks to the error field (see Sec. III D). In all cases, the locking and unlocking bifurcations are similar to those by which a tearing mode locks to and unlocks from an error field in a tokamak.[13] As always, there is considerable hysteresis in the locking/unlocking process, since the locking thresholds [given in Eq. (163)] are much smaller than the corresponding unlocking thresholds [given in Eqs. (167) and (168)]. Furthermore, as described in Sec. III C, the criteria for the formation and breakup of the slinky mode are slightly modified when the reversal surface is locked to an error field.

The dominant error-field source in a RFP is usually a 1,0 field arising from the mismatch between the ''vertical'' magnetic fields interior and exterior to the conducting shell. Of course, the plasma experiences this field filtered through the gaps in the shell. In Sec. III E, it is demonstrated that if the shell contains a single poloidal gap and a single toroidal gap then the slinky mode only locks to the poloidal gap when the ''vertical'' error field points toward the toroidal gap. If there is a mismatch between the direction of the ''vertical'' error field and the poloidal location of the toroidal gap, then there is a corresponding mismatch between the locking angle of the slinky mode and the toroidal location of the poloidal gap. This calculation can be generalized to take account of more complicated gap arrangements in a fairly straightforward manner.

Finally, in Sec. III F we discuss two methods for alleviating the problems associated with a locked slinky mode. The first, and most obvious, method is to cancel out the accidentally produced error field responsible for locking the

slinky mode using a deliberately generated ''control'' error field. It is assumed that the control field is a 0,1 perturbation (in the absence of the plasma and the conducting shell). It is found that the amplitude of the locking field is most effectively minimized when the control field is in *antiphase* with the locking phase of the slinky mode. If the amplitude of the control field is adjusted such that the locking field is made sufficiently small, then a bifurcation is triggered by which the slinky mode either unlocks, and starts to rotate, or breaks up altogether. The unlocking threshold is specified in Eqs. (167) and (168), whereas the breakup threshold is determined by Eq. (146). The second, and more practical, method is to sweep the locking angle of the slinky mode toroidally using a rotating control field. It is demonstrated that if the amplitude of the control field is too low, then the locking angle merely oscillates about its unperturbed value. However, above a certain critical value of this amplitude the locking angle executes complete toroidal rotations around the device at the angular oscillation frequency of the control field.

V. KEY RESULTS

The key new results of this paper are the following.

(i)   Equations (A77), (A99)–(A101), and (A104)–(A106), which describe the nonlinear electromagnetic coupling of the various different $m = 1$ dynamo modes in a RFP. The nonlinear terms are calculated via *quasilinear* theory (i.e., using *liner* eigenfunctions). This weakly nonlinear approach is justified during the sawtooth ramp phases of a RFP discharge: i.e., when the highly nonlinear MHD dynamo is not active.

(ii)   Equations (67), which are a collection of nonlinear equations governing the phase relations of a set of saturated rotating dynamo modes subject to nonlinear electromagnetic locking torques and viscous restoring torques. The solution of these equations describes how the slinky mode forms via a series of bifurcations as the typical mode amplitude is increased.

(iii)   Equations (72), which are a collection of nonlinear equations governing the phase relations of a set of saturated dynamo modes that are phase locked together so as to form a rotating slinky mode. The solution of these equations describes how the slinky mode breaks up via a series of bifurcations as the typical mode amplitude is decreased.

(iv)   Equations (161) and (166), which describe the locking and unlocking, respectively, of a rotating slinky mode to a static error field.

APPENDIX A: NONLINEAR COUPLING

1. The plasma equilibrium

Consider a large aspect ratio,[21] zero-β,[22] RFP plasma equilibrium whose unperturbed magnetic flux surfaces map out (almost) concentric circles in the poloidal plane. Such an equilibrium is well approximated as a periodic cylinder. Suppose that the minor radius of the plasma is a. Standard cylindrical polar coordinates (r,θ,z) are adopted. The system is assumed to be periodic in the z direction, with periodicity length $2\pi R_0$, where R_0 is the simulated major radius of the plasma. It is convenient to define a simulated toroidal angle $\phi = z/R_0$.

The equilibrium magnetic field is written as

$$\mathbf{B} = [0, B_\theta(r), B_\phi(r)]. \tag{A1}$$

The associated equilibrium plasma current takes the form

$$\mu_0 \mathbf{J} = [0, -B_\phi', (rB_\theta)'/r], \tag{A2}$$

where $'$ denotes d/dr. In a RFP $|B_\theta/B_\phi| \sim O(1)^2$.

The model RFP equilibrium used in this paper is the well-known α-Θ_0 model,[30] according to which

$$\nabla \wedge \mathbf{B} = \sigma(r)\mathbf{B}, \tag{A3}$$

where

$$\sigma = \left(\frac{2\Theta_0}{a}\right)\left[1 - \left(\frac{r}{a}\right)^\alpha\right]. \tag{A4}$$

Here, both α and Θ_0 are positive constants. Note that $\sigma = \text{const}$ (i.e., $\alpha \to \infty$) corresponds to a *Taylor state*.[3,31] In theory, a RFP equilibrium should relax to a Taylor state. In practice, relaxation occurs everywhere in the plasma apart from close to the edge, where the plasma is sufficiently cold and resistive that the strong equilibrium currents associated with a Taylor state cannot be maintained. Hence, α is finite. In general, Θ_0 is such that there is a *reversal surface*, where B_ϕ goes through zero, situated close to the plasma boundary.

2. The linear eigenmode equation

The linearized, marginally stable, ideal-MHD force balance equation takes the form

$$(\mathbf{j}\cdot\nabla)\mathbf{B} + (\mathbf{J}\cdot\nabla)\mathbf{b} - (\mathbf{b}\cdot\nabla)\mathbf{J} - (\mathbf{B}\cdot\nabla)\mathbf{j} = \mathbf{0}, \tag{A5}$$

where $\mathbf{b}$ and $\mathbf{j}$ are the perturbed magnetic field and plasma current, respectively.

A general perturbed quantity can be written as

$$\mathbf{a}(\mathbf{r},t) = \sum_{m,n} \mathbf{a}^{m,n}(r,t)e^{i(m\theta - n\phi)}, \tag{A6}$$

where m,n are integers. It is convenient to define

$$\psi^{m,n}(r,t) = -irb_r^{m,n}(r,t). \tag{A7}$$

It follows that

$$b_\theta^{m,n} = -\frac{m(\psi^{m,n})'}{m^2 + n^2\epsilon^2} + \frac{n\epsilon\sigma\psi^{m,n}}{m^2 + n^2\epsilon^2}, \tag{A8}$$

$$b_\phi^{m,n} = \frac{n\epsilon(\psi^{m,n})'}{m^2 + n^2\epsilon^2} + \frac{m\sigma\psi^{m,n}}{m^2 + n^2\epsilon^2}, \tag{A9}$$

and

$$\mu_0 \mathbf{j}^{m,n} = \sigma\mathbf{b}^{m,n} + \frac{ir\sigma' b_r^{m,n}}{mB_\theta - n\epsilon B_\phi}\mathbf{B}. \tag{A10}$$

Here,

$$\epsilon(r) = \frac{r}{R_0}. \tag{A11}$$

In a large aspect ratio RFP, $\epsilon \ll 1$ and $m \sim n\epsilon \sim O(1)$.[32]

Equation (A5) reduces to the well-known eigenmode equation[33]

$$\frac{d}{dr}\left(f^{m,n}\frac{d\psi^{m,n}}{dr}\right) - g^{m,n}\psi^{m,n} = 0, \tag{A12}$$

where

$$f^{m,n}(r) = \frac{r}{m^2 + n^2\epsilon^2}, \tag{A13}$$

$$g^{m,n}(r) = \frac{1}{r} + \frac{r(n\epsilon B_\theta + mB_\phi)}{(m^2 + n^2\epsilon^2)(mB_\theta - n\epsilon B_\phi)}\frac{d\sigma}{dr}$$
$$+ \frac{2mn\epsilon\sigma}{(m^2 + n^2\epsilon^2)^2} - \frac{r\sigma^2}{m^2 + n^2\epsilon^2}. \tag{A14}$$

In the limit $r \to 0$, a regular solution to Eq. (A12) satisfies $\psi^{m,n} \sim r^{|m|}$ for $m \neq 0$, and $\psi^{m,n} \sim r^2$ for the special case $m = 0$.

Suppose that the plasma is surrounded by a vacuum gap, extending over the region $a < r < b$, which is bounded by a perfectly conducting shell situated at $r = b$. It follows that $\sigma(r) = 0$ for $a < r < b$, and

$$\psi^{m,n}(b) = 0. \tag{A15}$$

3. Resonant modes

Let

$$F^{m,n}(r) = mB_\theta - n\epsilon B_\phi, \tag{A16}$$

$$G^{m,n}(r) = n\epsilon B_\theta + mB_\phi, \tag{A17}$$

$$H^{m,n}(r) = m^2 + n^2\epsilon^2. \tag{A18}$$

A *resonant* mode satisfies

$$F^{m,n}(r_s^{m,n}) = 0, \tag{A19}$$

for $0 < r_s^{m,n} < a$. The flux surface $r = r_s^{m,n}$ is known as the m,n mode *rational surface*.

Note that the eigenmode equation (A12) becomes *singular* at the m,n rational surface. The most general solution in the immediate vicinity of this surface takes the form

$$\psi^{m,n}(x) = C_L^{m,n}[1 + \lambda^{m,n}x(\ln|x| - 1) + \cdots]$$
$$+ C_S^{m,n}[x + \cdots], \tag{A20}$$

where

$$x = \frac{r - r_s^{m,n}}{r_s^{m,n}}, \tag{A21}$$

$$\lambda^{m,n} = \left(\frac{G^{m,n} r^2 \sigma'}{r(F^{m,n})'} \right)_{r_s^{m,n}},$$

$$x = \left(\frac{r \sigma'}{\sigma} \right)_{r_s^{\min}}. \tag{A22}$$

Here, $C_L^{m,n}$ and $C_S^{m,n}$ are known as the coefficients of the large and small solutions, respectively.

In a zero-β plasma it is possible to demonstrate that the coefficient of the large solution must be continuous across a mode rational surface, whereas the coefficient of the small solution may be discontinuous.[20,26] Thus, the m,n mode can be characterized by two complex parameters:

$$\Psi^{m,n} = C_L^{m,n}, \tag{A23}$$

$$\Delta \Psi^{m,n} = [C_S]_{r_s^{m,n}-}^{r_s^{m,n}+}. \tag{A24}$$

The m,n eigenfunction can be written as

$$\psi^{m,n}(r,t) = \Psi^{m,n}(t) \hat{\psi}^{m,n}(r), \tag{A25}$$

where $\hat{\psi}^{m,n}$ is a real solution of Eq. (A12), which is regular at $r=0$, satisfies the boundary condition (A15), and is continuous at the rational surface. In addition,

$$\hat{\psi}^{m,n}(r_s^{m,n}) = 1. \tag{A26}$$

Incidentally, the boundary condition (A15) is equivalent to

$$\left(\frac{r}{\hat{\psi}^{m,n}} \frac{d\hat{\psi}^{m,n}}{dr} \right)_a = \kappa^{m,n}, \tag{A27}$$

where

$$\kappa^{m,n} = \frac{m^2 + n^2 \epsilon_a^2}{n \epsilon_a} \frac{I_m(n\epsilon_a) K_m'(n\epsilon_b) - K_m(n\epsilon_a) I_m'(n\epsilon_b)}{I_m'(n\epsilon_a) K_m'(n\epsilon_b) - K_m'(n\epsilon_a) I_m'(n\epsilon_b)}. \tag{A28}$$

Here, $\epsilon_a = a/R_0$, $\epsilon_b = b/R_0$, and I_m, K_m are modified Bessel functions. Note that $I_m'(z) \equiv dI_m(z)/dz$, etc.

In general, $\hat{\psi}^{m,n}$ possesses a gradient discontinuity at the rational surface. This discontinuity is conveniently parametrized by

$$E^{m,n} = \left(r \frac{d\hat{\psi}^{m,n}}{dr} \right)_{r_s^{m,n}-}^{r_s^{m,n}+}. \tag{A29}$$

Note that $E^{m,n}$ is a real number.

As is well known, in a zero-β plasma the m,n mode is resistively unstable whenever $E^{m,n} > 0$, and is stable otherwise.[34] This type of instability is known as a *tearing mode*, since in its nonlinear phase it "tears" and reconnects the equilibrium magnetic field.[19] Likewise, $E^{m,n}$ is known as the *tearing stability index* for the m,n mode, and $\psi^{m,n}(r,t)$ is the associated *tearing eigenfunction*.

4. Nonresonant modes

A nonresonant mode (i.e., a mode possessing no rational surface inside the plasma) cannot be resistively unstable, but may be ideally unstable. For such a mode, it is possible to define an *ideal stability index*,

$$E_*^{m,n} = \kappa^{m,n} - \left(\frac{r}{\psi^{m,n}} \frac{d\psi^{m,n}}{dr} \right)_a, \tag{A30}$$

assuming that $\psi^{m,n}$ is regular at $r=0$. It is easily demonstrated that the m,n mode is ideally unstable if $E_*^{m,n} > 0$, and is stable otherwise.[33]

In this paper, it is assumed that all nonresonant modes are ideally stable. This is always the case, provided that the flux conserving shell is situated sufficiently close to the edge of the plasma.[35]

5. Linear layer theory

Ideal MHD breaks down in the immediate vicinity of the m,n mode rational surface. In this region, nonideal effects such as plasma inertia, resistivity, and viscosity become important. Suppose that

$$\Psi^{m,n}(t) = \hat{\Psi}^{m,n} e^{i(\varphi^{m,n} - \omega^{m,n} t)}, \tag{A31}$$

where $\hat{\Psi}^{m,n}$, $\varphi^{m,n}$, and $\omega^{m,n}$ are real constants. Of course, $\omega^{m,n}$ is the *real frequency* of the m,n mode. Asymptotic matching between the thin layer, centered on the rational surface, where ideal MHD breaks down, and the remainder of the plasma, where ideal MHD is valid, yields

$$\Delta \Psi^{m,n} = \Delta^{m,n}(\omega^{m,n}) \Psi^{m,n}. \tag{A32}$$

Here, the complex parameter $\Delta^{m,n}$ is termed the *layer response function*.

In the so-called *viscoresistive* regime, the layer response function takes the form

$$\Delta^{m,n}(\omega^{m,n}) = 2.104 \, \omega^{m,n} \frac{(\tau_H^{m,n})^{1/3} (\tau_R^{m,n})^{5/6}}{(\tau_V^{m,n})^{1/6}} e^{-i\pi/2}, \tag{A33}$$

where

$$\tau_H^{m,n} = \left(\frac{\mu_0 \rho}{(F^{m,n})'^2} \right)_{r_s^{m,n}}^{1/2}, \tag{A34}$$

$$\tau_R^{m,n} = \left(\frac{\mu_0 r^2}{\eta} \right)_{r_s^{m,n}}, \tag{A35}$$

$$\tau_V^{m,n} = \left(\frac{\rho r^2}{\mu} \right)_{r_s^{m,n}}, \tag{A36}$$

are the hydromagnetic, resistive, and viscous time scales, respectively, evaluated at the m,n rational surface. Here, $\rho(r)$, $\eta(r)$, and $\mu(r)$ are the plasma mass density, (parallel) resistivity, and (perpendicular) viscosity, respectively. The criteria for the validity of the viscoresistive regime are set out in detail in Ref. 13.

6. Nonlinear island theory

The nonlinear concomitant of the linear response regime discussed above is the well-known Rutherford regime.[19] A straightforward generalization of Rutherford's analysis (which makes ordering assumptions that are appropriate to tokamaks, but not to REPs) yields the following island width evolution equation:

$$I\tau_R^{m,n}\frac{d}{dt}\left(\frac{W^{m,n}}{r_s^{m,n}}\right)=\mathrm{Re}\left(\frac{\Delta\Psi^{m,n}}{\Psi^{m,n}}\right), \tag{A37}$$

where $I=0.8227$. Here,

$$W^{m,n}=4\left(\frac{|\Psi^{m,n}|}{|(F^{m,n})'|_{r_s^{m,n}}}\right)^{1/2} \tag{A38}$$

is the maximum radial width of the island chain at the m,n rational surface. Let

$$\zeta^{m,n}=m\theta-n\phi+\varphi^{m,n}-\omega^{m,n}t. \tag{A39}$$

For $dF^{m,n}(r_s^{m,n})/dr>0$, the X points of the island chain are situated at $\zeta^{m,n}=(2k-1)\pi$, and the O points are at $\zeta^{m,n}=2k\pi$, where k is an integer. For $dF^{m,n}(r_s^{m,n})/dr<0$, the O points are situated at $\zeta^{m,n}=(2k-1)\pi$, with the X points at $\zeta^{m,n}=2k\pi$. Note that $(F^{m,n})'>0$ for conventional RFP equilibria (assuming that $n\geq 0$).

The Rutherford regime takes over from the viscoresistive regime whenever the island width, $W^{m,n}$, exceeds the linear layer width,

$$\delta^{m,n}\sim\frac{(\tau_H^{m,n})^{1/3}}{(\tau_V^{m,n})^{1/6}(\tau_R^{m,n})^{1/6}}r_s^{m,n}. \tag{A40}$$

The criteria for the validity of the Rutherford regime are set out in detail in Ref. 13.

7. The nonlinear eigenmode equation

The complete, marginally stable, ideal-MHD force balance equation takes the form

$$(\mathbf{j}\cdot\mathbf{\nabla})\mathbf{B}+(\mathbf{J}\cdot\mathbf{\nabla})\mathbf{b}-(\mathbf{b}\cdot\mathbf{\nabla})\mathbf{J}-(\mathbf{B}\cdot\mathbf{\nabla})\mathbf{j}=\frac{\mathbf{A}}{\mu_0}, \tag{A41}$$

where

$$\mathbf{A}=\mu_0(\mathbf{b}\cdot\mathbf{\nabla})\mathbf{j}-\mu_0(\mathbf{j}\cdot\mathbf{\nabla})\mathbf{b}. \tag{A42}$$

Equation (A7) remains valid. However, Eqs. (A8)–(A10) generalize to

$$b_\theta^{m,n}=-\frac{m(\psi^{m,n})'}{H^{m,n}}+\frac{n\epsilon\sigma\psi^{m,n}}{H^{m,n}}+\frac{n\epsilon r^2 A_r^{m,n}}{H^{m,n}F^{m,n}}, \tag{A43}$$

$$b_\phi^{m,n}=\frac{n\epsilon(\psi^{m,n})'}{H^{m,n}}+\frac{m\sigma\psi^{m,n}}{H^{m,n}}+\frac{mr^2 A_r^{m,n}}{H^{m,n}F^{m,n}}, \tag{A44}$$

and

$$\mu_0 j_r^{m,n}=\sigma b_r^{m,n}+\frac{irA_r^{m,n}}{F^{m,n}}, \tag{A45}$$

$$\mu_0 j_\theta^{m,n}=\sigma b_\theta^{m,n}+\frac{ir\sigma'B_\theta b_\tau^{m,n}}{F^{m,n}}+\frac{irA_\theta^{m,n}}{F^{m,n}}$$
$$+\frac{r(r\sigma B_\phi-2B_\theta)A_r^{m,n}}{(F^{m,n})^2}, \tag{A46}$$

$$\mu_0 j_\phi^{m,n}=\sigma b_\phi^{m,n}+\frac{ir\sigma'B_\phi b_r^{m,n}}{F^{m,n}}+\frac{irA_\phi^{m,n}}{F^{m,n}}-\frac{r^2\sigma B_\theta A_r^{m,n}}{(F_{m,n})^2}. \tag{A47}$$

Likewise, Eq. (A12) generalizes to

$$\frac{d}{dr}\left(f^{m,n}\frac{d\psi^{m,n}}{dr}\right)-g^{m,n}\psi^{m,n}=\frac{U^{m,n}}{m}=\frac{V^{m,n}}{n\epsilon}, \tag{A48}$$

where

$$U^{m,n}=-i\frac{r^2 A_\phi^{m,n}}{F^{m,n}}+\frac{n\epsilon r^3\sigma G^{m,n}A_r^{m,n}}{H^{m,n}(F^{m,n})^2}+\left(\frac{n\epsilon r^3 A_r^{m,n}}{H^{m,n}F^{m,n}}\right)', \tag{A49}$$

$$V^{m,n}=-i\frac{r^2 A_\theta^{m,n}}{F^{m,n}}+\frac{2r^2 B_\theta A_r^{m,n}}{(F^{m,n})^2}-\frac{mr^3\sigma G^{m,n}A_r^{m,n}}{H^{m,n}(F^{m,n})^2}$$
$$-r\left(\frac{mr^2 A_r^{m,n}}{H^{m,n}F^{m,n}}\right)'. \tag{A50}$$

8. The nonlinear coupling coefficients

Consider the nonlinear coupling of *three* tearing modes with mode numbers m_1,n_1; m_2,n_2; and m_3,n_3, where

$$m_3=m_1+m_2, \tag{A51}$$

$$n_3=n_1+n_2. \tag{A52}$$

It can be demonstrated, after considerable algebra, that

$$A_r^{m_1,n_1}=-(\Psi^{m_2,n_2})^*\Psi^{m_3,n_3}\frac{\sigma'\hat{\psi}^{m_2,n_2}\hat{\psi}^{m_3,n_3}}{4r^2}\frac{(F^{m_1,n_1})^2}{F^{m_2,n_2}F^{m_3,n_3}}, \tag{A53}$$

$$A_r^{m_2,n_2}=-(\Psi^{m_1,n_1})^*\Psi^{m_3,n_3}\frac{\sigma'\hat{\psi}^{m_1,n_1}\hat{\psi}^{m_3,n_3}}{4r^2}\frac{(F^{m_2,n_2})^2}{F^{m_1,n_2}F^{m_3,n_3}}, \tag{A54}$$

$$A_r^{m_3,n_3}=-\Psi^{m_1,n_1}\Psi^{m_2,n_2}\frac{\sigma'\hat{\psi}^{m_1,n_1}\hat{\psi}^{m_2,n_2}}{4r^2}\frac{(F^{m_3,n_3})^2}{F^{m_1,n_1}F^{m_2,n_2}}. \tag{A55}$$

Likewise,

$$
A_\theta^{m_1,n_1} = i(\Psi^{m_2,n_2})^* \Psi^{m_3,n_3} \frac{\sigma'}{4} \left[\frac{\hat\psi^{m_2,n_2}(\hat\psi^{m_3,n_3})'}{r} \frac{n_1 \epsilon G^{m_3,n_3}}{H^{m_3,n_3} F^{m_2,n_2}} + \frac{\hat\psi^{m_3,n_3}(\hat\psi^{m_2,n_2})'}{r} \frac{n_1 \epsilon G^{m_2,n_2}}{H^{m_2,n_2} F^{m_3,n_3}} \right.
$$
$$
\left. + \frac{n_1 \epsilon \sigma \hat\psi^{m_2,n_2}\hat\psi^{m_3,n_3}}{r} \left(\frac{F^{m_2,n_2}}{H^{m_2,n_2} F^{m_3,n_3}} + \frac{F^{m_3,n_3}}{H^{m_3,n_3} F^{m_2,n_2}} \right) - \frac{1}{\sigma'} \left(\frac{\sigma' B_\theta F^{m_1,n_1} \hat\psi^{m_2,n_2}\hat\psi^{m_3,n_3}}{r F^{m_2,n_2} F^{m_3,n_3}} \right)' \right],
\tag{A56}
$$

$$
A_\theta^{m_2,n_2} = i(\Psi^{m_1,n_1})^* \Psi^{m_3,n_3} \frac{\sigma'}{4} \left[\frac{\hat\psi^{m_1,n_1}(\hat\psi^{m_3,n_3})'}{r} \frac{n_2 \epsilon G^{m_3,n_3}}{H^{m_3,n_3} F^{m_1,n_1}} + \frac{\hat\psi^{m_3,n_3}(\hat\psi^{m_1,n_1})'}{r} \frac{n_2 \epsilon G^{m_1,n_1}}{H^{m_1,n_1} F^{m_3,n_3}} \right.
$$
$$
\left. + \frac{n_2 \epsilon \sigma \hat\psi^{m_1,n_1}\hat\psi^{m_3,n_3}}{r} \left(\frac{F^{m_1,n_1}}{H^{m_1,n_1} F^{m_3,n_3}} + \frac{F^{m_3,n_3}}{H^{m_3,n_3} F^{m_1,n_1}} \right) - \frac{1}{\sigma'} \left(\frac{\sigma' B_\theta F^{m_2,n_2} \hat\psi^{m_1,n_1}\hat\psi^{m_3,n_3}}{r F^{m_1,n_1} F^{m_3,n_3}} \right)' \right],
\tag{A57}
$$

$$
A_\theta^{m_3,n_3} = i\Psi^{m_1,n_1} \Psi^{m_2,n_2} \frac{\sigma'}{4} \left[\frac{\hat\psi^{m_1,n_1}(\hat\psi^{m_2,n_2})'}{r} \frac{n_3 \epsilon G^{m_2,n_2}}{H^{m_2,n_2} F^{m_1,n_1}} + \frac{\hat\psi^{m_2,n_2}(\hat\psi^{m_1,n_1})'}{r} \frac{n_3 \epsilon G^{m_1,n_1}}{H^{m_1,n_1} F^{m_2,n_2}} \right.
$$
$$
\left. + \frac{n_3 \epsilon \sigma \hat\psi^{m_1,n_1}\hat\psi^{m_2,n_2}}{r} \left(\frac{F^{m_1,n_1}}{H^{m_1,n_1} F^{m_2,n_2}} + \frac{F^{m_2,n_2}}{H^{m_2,n_2} F^{m_1,n_1}} \right) - \frac{1}{\sigma'} \left(\frac{\sigma' B_\theta F^{m_3,n_3} \hat\psi^{m_1,n_1}\hat\psi^{m_2,n_2}}{r F^{m_1,n_1} F^{m_2,n_2}} \right)' \right],
\tag{A58}
$$

Finally,

$$
A_\phi^{m_1,n_1} = i(\Psi^{m_2,n_2})^* \Psi^{m_3,n_3} \frac{\sigma'}{4} \left[\frac{\hat\psi^{m_2,n_2}(\hat\psi^{m_3,n_3})'}{r} \frac{m_1 G^{m_3,n_3}}{H^{m_3,n_3} F^{m_2,n_2}} + \frac{\hat\psi^{m_3,n_3}(\hat\psi^{m_2,n_2})'}{r} \frac{m_1 G^{m_2,n_2}}{H^{m_2,n_2} F^{m_3,n_3}} \right.
$$
$$
\left. + \frac{m_1 \sigma \hat\psi^{m_2,n_2}\hat\psi^{m_3,n_3}}{r} \left(\frac{F^{m_2,n_2}}{H^{m_2,n_2} F^{m_3,n_3}} + \frac{F^{m_3,n_3}}{H^{m_3,n_3} F^{m_2,n_2}} \right) - \frac{1}{r\sigma'} \left(\frac{\sigma' B_\phi F^{m_1,n_1} \hat\psi^{m_2,n_2}\hat\psi^{m_3,n_3}}{F^{m_2,n_2} F^{m_3,n_3}} \right)' \right],
\tag{A59}
$$

$$
A_\phi^{m_2,n_2} = i(\Psi^{m_1,n_1})^* \Psi^{m_3,n_3} \frac{\sigma'}{4} \left[\frac{\hat\psi^{m_1,n_1}(\hat\psi^{m_3,n_3})'}{r} \frac{m_2 G^{m_3,n_3}}{H^{m_3,n_3} F^{m_1,n_1}} + \frac{\hat\psi^{m_3,n_3}(\hat\psi^{m_1,n_1})'}{r} \frac{m_2 G^{m_1,n_1}}{H^{m_1,n_1} F^{m_3,n_3}} \right.
$$
$$
\left. + \frac{m_2 \sigma \hat\psi^{m_1,n_1}\hat\psi^{m_3,n_3}}{r} \left(\frac{F^{m_1,n_1}}{H^{m_1,n_1} F^{m_3,n_3}} + \frac{F^{m_3,n_3}}{H^{m_3,n_3} F^{m_1,n_1}} \right) - \frac{1}{r\sigma'} \left(\frac{\sigma' B_\phi F^{m_2,n_2} \hat\psi^{m_1,n_1}\hat\psi^{m_3,n_3}}{F^{m_1,n_1} F^{m_3,n_3}} \right)' \right],
\tag{A60}
$$

$$
A_\phi^{m_3,n_3} = i\Psi^{m_1,n_1} \Psi^{m_2,n_2} \frac{\sigma'}{4} \left[\frac{\hat\psi^{m_1,n_1}(\hat\psi^{m_2,n_2})'}{r} \frac{m_3 G^{m_2,n_2}}{H^{m_2,n_2} F^{m_1,n_1}} + \frac{\hat\psi^{m_2,n_2}(\hat\psi^{m_1,n_1})'}{r} \frac{m_3 G^{m_1,n_1}}{H^{m_1,n_1} F^{m_2,n_2}} \right.
$$
$$
\left. + \frac{m_3 \sigma \hat\psi^{m_1,n_1}\hat\psi^{m_2,n_2}}{r} \left(\frac{F^{m_1,n_1}}{H^{m_1,n_1} F^{m_2,n_2}} + \frac{F^{m_2,n_2}}{H^{m_2,n_2} F^{m_1,n_1}} \right) - \frac{1}{r\sigma'} \left(\frac{\sigma' B_\phi F^{m_3,n_3} \hat\psi^{m_1,n_1}\hat\psi^{m_2,n_2}}{F^{m_1,n_1} F^{m_2,n_2}} \right)' \right].
\tag{A61}
$$

Incidentally, since $\nabla \cdot \mathbf{A} = 0$, it follows that

$$
\frac{d(rA_r^{m,n})}{dr} + im A_\theta^{m,n} - in\epsilon A_\phi^{m,n} = 0.
\tag{A62}
$$

It is easily verified that the expressions (A53)–(A61) respect this constraint.

9. Electromagnetic torques

The flux-surface-averaged poloidal and toroidal electromagnetic torques acting on the plasma are written as

$$
T_{\theta\ \mathrm{EM}}(r) = \frac{\pi^2 R_0}{\mu_0} \frac{d}{dr}\left(\sum_{m,n} r^2 [b_r^{m,n}(b_\theta^{m,n})^* + (b_r^{m,n})^* b_\theta^{m,n}] \right),
\tag{A63}
$$

$$
T_{\phi\ \mathrm{EM}}(r) = \frac{\pi^2 R_0^2}{\mu_0} \frac{d}{dr}\left(\sum_{m,n} r[b_r^{m,n}(b_\phi^{m,n})^* + (b_r^{m,n})^* b_\phi^{m,n}] \right),
\tag{A64}
$$

respectively. These expressions reduce to

$$
T_{\theta\ \mathrm{EM}}(r) = \frac{\pi^2 R_0}{\mu_0} \frac{d}{dr}\left(\sum_{m,n} W_\theta^{m,n} \right),
\tag{A65}
$$

$$
T_{\phi\ \mathrm{EM}}(r) = -\frac{\pi^2 R_0}{\mu_0} \frac{d}{dr}\left(\sum_{m,n} W_\phi^{m,n} \right),
\tag{A66}
$$

where

$$W_\theta^{m,n}(r) = i\left(m f^{m,n}(\psi^{m,n})'(\psi^{m,n})^* - \frac{n\epsilon r^3 A_r^{m,n}(\psi^{m,n})^*}{H^{m,n}F^{m,n}} \right)$$
$$+ \text{c.c.}, \tag{A67}$$

$$W_\phi^{m,n}(r) = i\left(n f^{m,n}(\psi^{m,n})'(\psi^{m,n})^* + \frac{m r^2 R_0 A_r^{m,n}(\psi^{m,n})^*}{H^{m,n}F^{m,n}} \right)$$
$$+ \text{c.c.} \tag{A68}$$

It follows from Eq. (A48) that

$$(W_\theta^{m,n})' = i U^{m,n}(\psi^{m,n})^* - i\left(\frac{n\epsilon r^3 A_r^{m,n}(\psi^{m,n})^*}{H^{m,n}F^{m,n}} \right)' + \text{c.c.}, \tag{A69}$$

$$(W_\phi^{m,n})' = i \frac{V^{m,n}(\psi^{m,n})^*}{\epsilon} + i\left(\frac{m r^2 R_0 A_r^{m,n}(\psi^{m,n})^*}{H^{m,n}F^{m,n}} \right)' + \text{c.c.} \tag{A70}$$

Consider the nonlinear interaction of the m_1,n_1; m_2,n_2; and m_3,n_3 tearing modes, where the various mode numbers are related according to Eqs. (A51)–(A52). It can be demonstrated, after considerable algebra, that

$$(W_\theta^{m_1,n_1})' = \frac{1}{2}\text{Im}[(\Psi^{m_1,n_1}\Psi^{m_2,n_2})^*\Psi^{m_3,n_3}]$$
$$\times\left[-m_1 t(r) + \left(\frac{r\sigma' B_\phi \hat{\psi}^{m_1,n_1}\hat{\psi}^{m_2,n_2}\hat{\psi}^{m_3,n_3}}{F^{m_2,n_2}F^{m_3,n_3}} \right)' \right], \tag{A71}$$

$$(W_\theta^{m_2,n_2})' = \frac{1}{2}\text{Im}[(\Psi^{m_1,n_1}\Psi^{m_2,n_2})^*\Psi^{m_3,n_3}]$$
$$\times\left[-m_2 t(r) + \left(\frac{r\sigma' B_\phi \hat{\psi}^{m_1,n_1}\hat{\psi}^{m_2,n_2}\hat{\psi}^{m_3,n_3}}{F^{m_1,n_1}F^{m_3,n_3}} \right)' \right], \tag{A72}$$

$$(W_\theta^{m_3,n_3})' = \frac{1}{2}\text{Im}[(\Psi^{m_1,n_1}\Psi^{m_2,n_2})^*\Psi^{m_3,n_3}]$$
$$\times\left[m_3 t(r) - \left(\frac{r\sigma' B_\phi \hat{\psi}^{m_1,n_1}\hat{\psi}^{m_2,n_2}\hat{\psi}^{m_3,n_3}}{F^{m_1,n_1}F^{m_2,n_2}} \right)' \right]. \tag{A73}$$

Likewise,

$$(W_\phi^{m_1,n_1})' = \frac{1}{2}\text{Im}[(\Psi^{m_1,n_1}\Psi^{m_2,n_2})^*\Psi^{m_3,n_3}]$$
$$\times\left[-n_1 t(r) + \left(\frac{r\sigma' B_\theta \hat{\psi}^{m_1,n_1}\hat{\psi}^{m_2,n_2}\hat{\psi}^{m_3,n_3}}{\epsilon F^{m_2,n_2}F^{m_3,n_3}} \right)' \right], \tag{A74}$$

$$(W_\phi^{m_2,n_2})' = \frac{1}{2}\text{Im}[(\Psi^{m_1,n_1}\Psi^{m_2,n_2})^*\Psi^{m_3,n_3}]$$
$$\times\left[-n_2 t(r) + \left(\frac{r\sigma' B_\theta \hat{\psi}^{m_1,n_1}\hat{\psi}^{m_2,n_2}\hat{\psi}^{m_3,n_3}}{\epsilon F^{m_1,n_1}F^{m_3,n_3}} \right)' \right], \tag{A75}$$

$$(W_\phi^{m_3,n_3})' = \frac{1}{2}\text{Im}[(\Psi^{m_1,n_1}\Psi^{m_2,n_2})^*\Psi^{m_3,n_3}]$$
$$\times\left[n_3 t(r) - \left(\frac{r\sigma' B_\theta \hat{\psi}^{m_1,n_1}\hat{\psi}^{m_2,n_2}\hat{\psi}^{m_3,n_3}}{\epsilon F^{m_1,n_1}F^{m_2,n_2}} \right)' \right]. \tag{A76}$$

Here,

$$t(r) = \sigma'\left\{ r(\hat{\psi}^{m_1,n_1})' \hat{\psi}^{m_2,n_2}\hat{\psi}^{m_3,n_3}\frac{G^{m_1,n_1}}{H^{m_1,n_1}F^{m_2,n_2}F^{m_3,n_3}} + \hat{\psi}^{m_1,n_1}r(\hat{\psi}^{m_2,n_2})'\hat{\psi}^{m_3,n_3}\frac{G^{m_2,n_2}}{H^{m_2,n_2}F^{m_1,n_1}F^{m_3,n_3}} \right.$$
$$+ \hat{\psi}^{m_1,n_1}\hat{\psi}^{m_2,n_2}r(\hat{\psi}^{m_3,n_3})'\frac{G^{m_3,n_3}}{H^{m_3,n_3}F^{m_1,n_1}F^{m_2,n_2}} + \hat{\psi}^{m_1,n_1}\hat{\psi}^{m_2,n_2}\hat{\psi}^{m_3,n_3}\left[r\sigma\left(\frac{F^{m_1,n_1}}{H^{m_1,n_1}F^{m_2,n_2}F^{m_3,n_3}} \right.\right.$$
$$\left.\left.\left. + \frac{F^{m_2,n_2}}{H^{m_2,n_2}F^{m_1,n_1}F^{m_3,n_3}} + \frac{F^{m_3,n_3}}{H^{m_3,n_3}F^{m_1,n_1}F^{m_2,n_2}} \right) + \frac{2B_\theta B_\phi - r\sigma(B_\theta^2 + B_\phi^2)}{F^{m_1,n_1}F^{m_2,n_2}F^{m_3,n_3}} \right] \right\}. \tag{A77}$$

Let

$$W_\theta = W_\theta^{m_1,n_1} + W_\theta^{m_2,n_2} + W_\theta^{m_3,n_3}, \tag{A78}$$

$$W_\phi = W_\phi^{m_1,n_1} + W_\phi^{m_2,n_2} + W_\phi^{m_3,n_3}. \tag{A79}$$

Recall, from Eqs. (A65)–(A66), that

$$T_{\theta\text{EM}}(r) = \frac{\pi^2 R_0}{\mu_0}(W_\theta)', \tag{A80}$$

$$T_{\phi\text{EM}}(r) = -\frac{\pi^2 R_0}{\mu_0}(W_\phi)'. \tag{A81}$$

However, it follows from Eqs. (A71)–(A76) that

$$(W_\theta)' = 0, \tag{A82}$$

$$(W_\phi)' = 0, \tag{A83}$$

where use has been made of Eqs. (A51)–(A52). Hence, *zero* flux-surface-averaged electromagnetic torque is exerted throughout the bulk of the plasma as a consequence of the nonlinear coupling of tearing modes. This is the expected result, since it is well known that zero flux-surface-averaged electromagnetic torque can be exerted in *any* region of the plasma governed by the equations of marginally stable ideal MHD.[11]

10. Localized electromagnetic torques

The above demonstration that nonlinear mode coupling gives rise to no electromagnetic torques is valid in all regions of the plasma governed by the equations of marginally stable ideal MHD. However, these equations break down in the immediate vicinity of the rational surfaces associated with the three coupled tearing modes, so it is still possible that *localized* electromagnetic torques can develop at these surfaces. This is indeed the case. The fact that $(\psi^{m,n})'$ is discontinuous across the m,n rational surface, whereas the $\psi^{m,n}$ and $(\psi^{m',n'})'$ (where $m',n' \neq m,n$) are continuous, implies that $W_\theta^{m,n}$ and $W_\phi^{m,n}$ are also discontinuous across this surface—see Eqs. (A67) and (A68). Thus, Eqs. (A65) and (A66) yield

$$T_{\theta\mathrm{EM}}(r) = \sum_{m,n} \delta T_{\theta\,\mathrm{EM}}^{m,n} \delta(r - r_s^{m,n}), \tag{A84}$$

$$T_{\phi\mathrm{EM}}(\tau) = \sum_{m,n} \delta T_{\phi\mathrm{EM}}^{m,n} \delta(r - r_s^{m,n}), \tag{A85}$$

where

$$\delta T_{\theta\mathrm{EM}}^{m,n} = \Delta W_\theta^{m,n}, \tag{A86}$$

$$\delta T_{\phi\mathrm{EM}}^{m,n} = -\Delta W_\phi^{m,n}. \tag{A87}$$

Here, $\Delta W_\theta^{m,n} \equiv W_\theta^{m,n}(r_{s+}^{m,n}) - W_\theta^{m,n}(r_{s-}^{m,n})$, etc., and it is understood that the delta functions represent the thin nonideal-MHD regions centered on each of the rational surfaces.

It follows from Eqs. (A67) and (A68) that $W_\theta^{m,n} \to 0$ and $W_\phi^{m,n} \to 0$ as $r \to 0$, assuming that the $\psi^{m,n}$ are regular at $r = 0$. Likewise, the boundary condition (A15) yields $W_\theta^{m,n} = W_\phi^{m,n} = 0$ at $r = b$. Thus, Eq. (A71) can be integrated to give

$$W_\theta^{m_1,n_1}(r) = \tfrac{1}{2}\mathrm{Im}[(\Psi^{m_1,n_1}\Psi^{m_2,n_2})^*\Psi^{m_3,n_3}]$$

$$\times \left(-m_1 \int_0^r t(r')dr' \right.$$

$$\left. + \frac{r\sigma' B_\phi \hat{\psi}^{m_1,n_1}\hat{\psi}^{m_2,n_2}\hat{\psi}^{m_3,n_3}}{F^{m_2,n_2}F^{m_2,n_2}} \right), \tag{A88}$$

for $0 < r < r_s^{m,n}$, and

$$W_\theta^{m_1,n_1}(r) = \tfrac{1}{2}\mathrm{Im}[(\Psi^{m_1,n_1}\Psi^{m_2,n_2})^*\Psi^{m_3,n_3}]$$

$$\times \left(m_1 \int_r^b t(r')dr' \right.$$

$$\left. + \frac{r\sigma' B_\phi \hat{\psi}^{m_1,n_1}\hat{\psi}^{m_2,n_2}\hat{\psi}^{m_3,n_3}}{F^{m_2,n_2}F^{m_3,n_3}} \right), \tag{A89}$$

for $r_s^{m,n} < r < b$. Clearly,

$$\Delta W_\theta^{m_1,n_1} = \tfrac{1}{2}\mathrm{Im}[(\Psi^{m_1,n_1}\Psi^{m_2,n_2})^*\Psi^{m_3,n_3}]m_1\int_0^b t(r)dr. \tag{A90}$$

After performing many calculations, similar to the above, the following expressions for the poloidal and toroidal electromagnetic torques acting at the three nonlinearly coupled rational surfaces are obtained:

$$\delta T_{\theta\mathrm{EM}}^{m_1,n_1} = \frac{\pi^2 R_0}{2\mu_0}\mathrm{Im}[(\Psi^{m_1,n_1}\Psi^{m_2,n_2})^*\Psi^{m_3,n_3}]m_1\int_0^a t(r)dr, \tag{A91}$$

$$\delta T_{\theta\mathrm{EM}}^{m_2,n_2} = \frac{\pi^2 R_0}{2\mu_0}\mathrm{Im}[(\Psi^{m_1,n_1}\Psi^{m_2,n_2})^*\Psi^{m_3,n_3}]m_2\int_0^a t(r)dr, \tag{A92}$$

$$\delta T_{\theta\mathrm{EM}}^{m_3,n_3} = -\frac{\pi^2 R_0}{2\mu_0}\mathrm{Im}[(\Psi^{m_1,n_1}\Psi^{m_2,n_2})^*\Psi^{m_3,n_3}]m_3$$

$$\times \int_0^a t(r)dr, \tag{A93}$$

and

$$\delta T_{\phi\mathrm{EM}}^{m_1,n_1} = -\frac{\pi^2 R_0}{2\mu_0}\mathrm{Im}[(\Psi^{m_1,n_1}\Psi^{m_2,n_2})^*\Psi^{m_3,n_3}]n_1$$

$$\times \int_0^a t(r)dr, \tag{A94}$$

$$\delta T_{\phi\mathrm{EM}}^{m_2,n_2} = -\frac{\pi^2 R_0}{2\mu_0}\mathrm{Im}[(\Psi^{m_1,n_1}\Psi^{m_2,n_2})^*\Psi^{m_3,n_3}]n_2$$

$$\times \int_0^a t(r)dr, \tag{A95}$$

$$\delta T_{\phi\mathrm{EM}}^{m_3,n_3} = \frac{\pi^2 R_0}{2\mu_0}\mathrm{Im}[(\Psi^{m_1,n_1}\Psi^{m_2,n_2})^*\Psi^{m_3,n_3}]n_3\int_0^a t(r)dr. \tag{A96}$$

Here, use has been made of Eqs. (A86) and (A87). Note that the upper limits of integration in all of the integrals involving $t(r)$ can be changed from b to a, because the function $t(r)$ is zero in the vacuum region outside the plasma (since $\sigma' = 0$ in this region). Note, also, that $\int_0^a t(r)dr$ is *finite*, despite the fact that $t(r)$ is singular at the three nonlinearly coupled rational surfaces, provided that this integral is evaluated by taking its Cauchy principal part with respect to these singularities.

According to Eqs. (A91)–(A96),

$$\delta T_{\theta\mathrm{EM}}^{m_1,n_1} + \delta T_{\theta\mathrm{EM}}^{m_2,n_2} + \delta T_{\theta\mathrm{EM}}^{m_3,n_3} = 0, \tag{A97}$$

$$\delta T_{\phi\text{EM}}^{m_1,n_1} + \delta T_{\phi\text{EM}}^{m_2,n_2} + \delta T_{\phi\text{EM}}^{m_3,n_3} = 0, \tag{A98}$$

where use has been made of Eqs. (A51)–(A52). In other words, the sum of all the localized nonlinear electromagnetic torques acting inside the plasma is *zero*, as is required by the conservation of angular momentum.

Equations (A91)–(A96) generalize in a fairly straightforward manner to the case where there are more than three nonlinearly coupled tearing modes in the plasma.

11. The nonlinear tearing mode dispersion relation

Consider the nonlinear coupling of the m_1,n_1; m_2,n_2; and m_3,n_3 tearing modes, where the various mode numbers are related according to Eqs. (A51)–(A52). The nonlinearly modified dispersion relations for the three modes take the form

$$\Delta\Psi^{m_1,n_1} = E^{m_1,n_1}\Psi^{m_1,n_1} + B^{m_1,n_1}, \tag{A99}$$

$$\Delta\Psi^{m_2,n_2} = E^{m_2,n_2}\Psi^{m_2,n_2} + B^{m_2,n_2}, \tag{A100}$$

$$\Delta\Psi^{m_3,n_3} = E^{m_3,n_3}\Psi^{m_3,n_3} + B^{m_3,n_3}, \tag{A101}$$

where B^{m_1,n_1}, B^{m_2,n_2}, etc. are the nonlinear corrections.

As is easily demonstrated,[11] the localized poloidal and toroidal electromagnetic torques acting in the vicinity of the m,n mode rational surface can be written as

$$\delta T_{\theta\text{EM}}^{m,n} = -\frac{2\pi^2 R_0}{\mu_0}\frac{m}{H^{m,n}(r_s^{m,n})}\text{Im}[\Delta\Psi^{m,n}(\Psi^{m,n})*], \tag{A102}$$

$$\delta T_{\phi\text{EM}}^{m,n} = \frac{2\pi^2 R_0}{\mu_0}\frac{n}{H^{m,n}(r_s^{m,n})}\text{Im}[\Delta\Psi^{m,n}(\Psi^{m,n})*], \tag{A103}$$

respectively. A comparison between Eqs. (A99)–(A103) and Eqs. (A91)–(A96) yields

$$B^{m_1,n_1} = -(\Psi^{m_2,n_2})*\Psi^{m_3,n_3}\frac{H^{m_1,n_1}(r_s^{m_1,n_1})}{4}\int_0^a t(r)dr, \tag{A104}$$

$$B^{m_2,n_2} = -(\Psi^{m_1,n_1})*\Psi^{m_3,n_3}\frac{H^{m_2,n_2}(r_s^{m_2,n_2})}{4}\int_0^a t(r)dr, \tag{A105}$$

$$B^{m_3,n_3} = -(\Psi^{m_1,n_1})\Psi^{m_2,n_2}\frac{H^{m_3,n_3}(r_s^{m_3,n_3})}{4}\int_0^a t(r)dr. \tag{A106}$$

The above expressions can be generalized in a fairly straightforward manner to the case where there are more than three nonlinearly coupled tearing modes in the plasma.

APPENDIX B: ERROR FIELDS

1. The tearing mode dispersion relation

In the presence of a static m,n error field the most general solution to Eq. (A12) is written as

$$\psi^{m,n}(r,t) = \Psi^{m,n}(t)\hat{\psi}^{m,n}(r) + C^{m,n}\tilde{\psi}^{m,n}(r), \tag{B1}$$

where $C^{m,n}$ is a complex parameter that specifies the amplitude and phase of the error field at the rational surface, and $\tilde{\psi}^{m,n}$ is a real function that specifies the *ideal* response of the plasma to the error field. To be more exact, $\tilde{\psi}^{m,n}(r)$ has the following properties:

$$\tilde{\psi}^{m,n} = 0, \quad \text{for } r \leqslant r_s^{m,n}, \tag{B2}$$

$$\left(\frac{r}{\tilde{\psi}^{m,n}}\frac{d\tilde{\psi}^{m,n}}{dr}\right)_{r_{s+}^{m,n}} = 1. \tag{B3}$$

Incidentally, the above definition completely specifies $\tilde{\psi}^{m,n}(r)$. Note that $\tilde{\psi}^{m,n}(b) \neq 0$, since the error field is assumed to leak through narrow gaps in the flux conserving shell.

Neglecting the nonlinear coupling of tearing modes, the error-field modified dispersion relation for the m,n tearing mode is written as

$$\Delta\Psi^{m,n} = E^{m,n}\Psi^{m,n} + C^{m,n}. \tag{B4}$$

It follows from Eqs. (A102)–(A103) that the poloidal and toroidal components of the electromagnetic torque exerted on the plasma in the immediate vicinity of the m,n rational surface by the m,n error field are given by

$$\delta T_{\theta\text{EM}}^{m,n} = -\frac{2\pi^2 R_0}{\mu_0}\frac{m}{H^{m,n}(r_s^{m,n})}\text{Im}[C^{m,n}(\Psi^{m,n})*], \tag{B5}$$

$$\delta T_{\phi\text{EM}}^{m,n} = \frac{2\pi^2 R_0}{\mu_0}\frac{n}{H^{m,n}(r_s^{m,n})}\text{Im}[C^{m,n}(\Psi^{m,n})*], \tag{B6}$$

respectively.

2. The vacuum region

In the vacuum region outside the plasma,

$$b_r^{m,n}(r) = \frac{i\psi^{m,n}(r,t)}{r}, \tag{B7}$$

$$b_\theta^{m,n}(r,t) = -\frac{m(\psi^{m,n})'}{m^2+n^2\epsilon^2}, \tag{B8}$$

$$b_\phi^{m,n}(r,t) = \frac{n\epsilon(\psi^{m,n})'}{m^2+n^2\epsilon^2}, \tag{B9}$$

where

$$\frac{d}{dr}\left(\frac{r}{m^2+n^2\epsilon^2}\frac{d\psi^{m,n}}{dr}\right) - \frac{\psi^{m,n}}{r} = 0. \tag{B10}$$

The most general solution to the above equation is

$$\psi^{m,n}(r) = a^{m,n}n\epsilon I_m'(n\epsilon) + b^{m,n}n\epsilon K_m'(n\epsilon). \tag{B11}$$

Here, the $a^{m,n}$ and $b^{m,n}$ are arbitrary complex constants. For the special case $n=0$, the above expression reduces to

$$\psi^{m,0}(r) = a^{m,0}r^{|m|} + b^{m,0}r^{-|m|}. \tag{B12}$$

3. Characterization of the error field

Suppose that, in the absence of the plasma and the flux-conserving shell, the error field is characterized by the mag-

netic streamfunction $\psi_{\text{ext}}(r,\theta,\phi)$. In the presence of the shell, but still in the absence of plasma, the m,n error field interior to the shell is characterized by

$$\psi^{m,n}(r) = \Psi^{m,n}_{\text{gap}} \hat{\psi}^{m,n}_{\text{gap}}(r), \tag{B13}$$

where

$$\hat{\psi}^{m,n}_{\text{gap}} = \frac{n\epsilon I'_m(n\epsilon)}{n\epsilon_b I'_m(n\epsilon_b)}, \tag{B14}$$

and

$$\Psi^{m,n}_{\text{gap}} = \int\int_{\text{gaps}} \psi_{\text{ext}}(b,\theta,\phi) e^{-i(m\theta - n\phi)} \frac{d\theta}{2\pi} \frac{d\phi}{2\pi}. \tag{B15}$$

The integral in the above expression is taken over the angular extent of the vacuum gaps in the shell. Here, the shell is naively modeled as a *filter* that does not modify b_r in the gaps, but requires $b_r = 0$ elsewhere. Note that in the special case $n = 0$,

$$\hat{\psi}^{m,0}_{\text{gap}} = \left(\frac{r}{b}\right)^{|m|}. \tag{B16}$$

In the presence of plasma, the m,n magnetic field in the vacuum region $a < r < b$ is characterized by

$$\psi^{m,n}(r) = \Psi^{m,n}_{\text{gap}} \hat{\psi}^{m,n}_{\text{gap}}(r) + \Psi^{m,n}_{\text{plasma}} \hat{\psi}^{m,n}_{\text{plasma}}(r), \tag{B17}$$

where

$$\hat{\psi}^{m,n}_{\text{plasma}}(r) = \frac{n\epsilon[K'_m(n\epsilon_b)I'_m(n\epsilon) - I'_m(n\epsilon_b)K'_m(n\epsilon)]}{n\epsilon_a[K'_m(n\epsilon_b)I'_m(n\epsilon_a) - I'_m(n\epsilon_b)K'_m(n\epsilon_a)]}. \tag{B18}$$

Here, $\Psi^{m,n}_{\text{plasma}}$ is a complex constant that parametrizes the amplitude and phase of the m,n plasma eigenfunction at $r = a$. Any leakage of the plasma eigenfunction through the gaps is neglected: this is only likely to be a good approximation if the gaps are relatively narrow. For the special case $n = 0$,

$$\hat{\psi}^{m,n}_{\text{plasma}}(r) = \frac{(r/b)^{|m|} - (r/b)^{-|m|}}{(a/b)^{|m|} - (a/b)^{-|m|}}. \tag{B19}$$

4. Electromagnetic torques

According to Eqs. (A65) and (A66), the total poloidal and toroidal electromagnetic torques acting on the plasma due to the m,n error field are

$$\delta T^{m,n}_{\theta\text{EM}} = -\frac{2\pi^2 R_0}{\mu_0} m \, \text{Im}[f^{m,n}(\psi^{m,n})'(\psi^{m,n})^*]_{a<r<b}, \tag{B20}$$

$$\delta T^{m,n}_{\phi\text{EM}} = \frac{2\pi^2 R_0}{\mu_0} n \, \text{Im}[f^{m,n}(\psi^{m,n})'(\psi^{m,n})^*]_{a<r<b}, \tag{B21}$$

respectively. Of course, these torques are exerted at the m,n rational surface.

It follows from Eq. (B17) that

$$[f^{m,n}(\psi^{m,n})'(\psi^{m,n})^*]_{a<r<b}$$
$$= \frac{\text{Im}[\Psi^{m,n}_{\text{gap}}(\Psi^{m,n}_{\text{plasma}})^*]}{(n\epsilon_a n\epsilon_b)[K'_m(n\epsilon_b)I'_m(n\epsilon_a) - I'_m(n\epsilon_b)K'_m(n\epsilon_a)]}. \tag{B22}$$

For the special case $n = 0$,

$$[f^{m,0}(\psi^{m,0})'(\psi^{m,0})^*]_{a<r<b}$$
$$= \frac{\text{Im}[\Psi^{m,0}_{\text{gap}}(\Psi^{m,0}_{\text{plasma}})^*]}{(|m|/2)[(b/a)^{|m|} - (b/a)^{-|m|}]}. \tag{B23}$$

5. Calculation of the error-field coupling constants

Equations (B1) and (B17) can be reconciled, provided that

$$\Psi^{m,n}_{\text{plasma}} = [\Psi^{m,n} - \Psi^{m,n}_{\text{gap}} \hat{\psi}^{m,n}_{\text{gap}}(r^{m,n}_s)] \hat{\psi}^{m,n}(a). \tag{B24}$$

It follows that

$$\text{Im}[\Psi^{m,n}_{\text{gap}}(\Psi^{m,n}_{\text{plasma}})^*] = \text{Im}[\Psi^{m,n}_{\text{gap}}(\Psi^{m,n})^*] \hat{\psi}^{m,n}(a). \tag{B25}$$

Thus, from Eqs. (B20) and (B22), the poloidal electromagnetic torque acting on the plasma takes the form

$$\delta T^{m,n}_{\theta\text{EM}} = -\frac{2\pi^2 R_0}{\mu_0} m$$
$$\times \frac{\text{Im}[\Psi^{m,n}_{\text{gap}}(\Psi^{m,n})^*] \hat{\psi}^{m,n}(a)}{(n\epsilon_a n\epsilon_b)[K'_m(n\epsilon_b)I'_m(n\epsilon_a) - I'_m(n\epsilon_b)K'_m(n\epsilon_a)]}. \tag{B26}$$

Finally, a comparison of the above expression with Eq. (B5) yields

$$C^{m,n} = c^{m,n}\Psi^{m,n}_{\text{gap}}, \tag{B27}$$

where the real parameter $c^{m,n}$ is written as

$$c^{m,n} = \frac{H^{m,n}(r^{m,n}_s)\hat{\psi}^{m,n}(a)}{(n\epsilon_a n\epsilon_b)[K'_m(n\epsilon_b)I'_m(n\epsilon_a) - I'_m(n\epsilon_b)K'_m(n\epsilon_a)]}. \tag{B28}$$

For the special case $n = 0$,

$$c^{m,0} = \frac{2|m|\hat{\psi}^{m,0}(a)}{(b/a)^{|m|} - (b/a)^{-|m|}}. \tag{B29}$$

6. Example error fields

The dominant error-field source in a RFP is usually the 1,0 field arising from the mismatch between the "vertical" magnetic fields interior and exterior to the shell. Let

$$\psi_{\text{ext}}(r,\theta,\phi) = B_v r^{i(\theta - \theta_v)}, \tag{B30}$$

which describes a uniform poloidal magnetic field, of magnitude B_v, directed toward $\theta = \theta_v$. Incidentally, in this paper $\theta = 0$ corresponds to the *inboard midplane* of the device.

Suppose that the flux-conserving shell contains two vacuum gaps: a *poloidal* gap, extending from $\phi = \phi_g$

$-\Delta\phi/2$ to $\phi=\phi_g+\Delta\phi/2$, and a *toroidal* gap, extending from $\theta=\theta_g-\Delta\theta/2$ to $\theta_g+\Delta\theta/2$. It follows from Eqs. (B15) and (B30) that for a 1,0 error field,

$$\Psi_{\mathrm{gap}}^{m,n}=B_v b f \operatorname{sinc}[(m-1)\Delta\theta/2]$$
$$\times \operatorname{sinc}[n\Delta\phi/2]e^{-i[(m-1)\theta_g+\theta_v-n\phi_g]}. \tag{B31}$$

Here, $\operatorname{sinc} x\equiv\sin x/x$, and $f=\Delta\theta\Delta\phi/4\pi^2$ is the area fraction of gaps.

The 0,1 error field is of particular significance in RFPs, since it resonates with the reversal surface, which controls the rotation of the slinky mode. Let

$$\psi_{\mathrm{ext}}(r,\theta,\phi)=B_c b\,\frac{\epsilon I_0'(\epsilon)}{\epsilon_b I_0'(\epsilon_b)}\,e^{-i(\phi-\phi_c)}, \tag{B32}$$

which describes a 0,1 field for which $b_r(b,\theta,\phi)$ attains its maximum amplitude, $b_r=B_c$, at $\phi=\phi_c$. It follows that

$$\Psi_{\mathrm{gap}}^{m,n}=B_c b f \operatorname{sinc}[m\Delta\theta/2]$$
$$\times \operatorname{sinc}[(n-1)\Delta\phi/2]e^{-i[m\theta_g-(n-1)\phi_g-\phi_c]}. \tag{B33}$$

[1] J. A. Wesson and D. J. Campbell, *Tokamaks*, 2nd ed. (Clarenden, Oxford, England, 1998).
[2] H. A. B. Bodin, Nucl. Fusion **30**, 1717 (1990).
[3] J. B. Taylor, Phys. Rev. Lett. **33**, 1139 (1974).
[4] R. N. Dexter, D. W. Kerst, T. W. Lovell, S. C. Prager, and J. C. Sprott, Fusion Technol. **19**, 131 (1991).
[5] A. F. Almagri, S. Assadi, S. C. Prager, J. S. Sarff, and D. W. Kerst, Phys. Fluids B **4**, 4080 (1992).
[6] R. J. La Haye, T. N. Carlstrom, R. R. Goforth *et al.* Phys. Fluids **27**, 2576 (1984).
[7] T. Tamano, W. D. Bard, C. Chu *et al.* Phys. Rev. Lett. **59**, 1444 (1987).
[8] K. Hattori, Y. Hirano, T. Shimada *et al.*, Phys. Fluids B **3**, 3111 (1991).
[9] V. Antoni, L. Apolloni, M. Bagatin *et al.*, in *Fusion Energy 1996*, Proceedings of the 16th International Conference, Montreal 1996 (International Atomic Energy Agency, Vienna, 1997), Vol. II, p. 711.
[10] F. Gnesotto *et al.*, Fusion Eng. Des. **25**, 335 (1995).
[11] R. Fitzpatrick, Nucl. Fusion **33**, 1049 (1993).
[12] R. Fitzpatrick, R. J. Hastie, T. J. Martin, and C. M. Roach, Nucl. Fusion **33**, 1533 (1993).
[13] R. Fitzpatrick, Phys. Plasmas **5**, 3325 (1998).
[14] D. D. Schnack and S. Ortolani, Nucl. Fusion **30**, 277 (1990).
[15] K. Kusano, T. Tamamo, and T. Sato, Nucl. Fusion **31**, 1923 (1991).
[16] C. C. Hegna, Phys. Plasmas **3**, 4646 (1996).
[17] J. S. Sarff, S. Assadi, and A. F. Almagri, Phys. Fluids B **5**, 2540 (1993).
[18] S. Ortolani and D. D. Schnack, *Magnetohydrodynamics of Plasma Relaxation* (World Scientific, Singapore, 1993).
[19] P. H. Rutherford, Phys. Fluids **16**, 1903 (1973).
[20] B. Coppi, J. M. Greene, and J. L. Johnson, Nucl. Fusion **6**, 101 (1966).
[21] The standard large aspect ratio ordering is $R_0/a\gg1$, where R_0 and a are the major and minor radii of the plasma, respectively.
[22] The conventional definition of this parameter is $\beta=2\mu_0\langle p\rangle/\langle B^2\rangle$, where $\langle\cdots\rangle$ denotes a volume average, p is the plasma pressure, and B is the magnetic field strength.
[23] T. H. Stix, Phys. Fluids **16**, 1260 (1973).
[24] C. G. Gimblett and R. S. Peckover, Proc. R. Soc. London, Ser. A **368**, 75 (1979).
[25] R. Fitzpatrick and T. C. Hender, Phys. Plasmas **1**, 3337 (1994).
[26] R. Fitzpatrick, Phys. Plasmas **1**, 3308 (1994).
[27] G. Fiksel, S. C. Prager, W. Shen, and M. R. Stoneking, Phys. Rev. Lett. **72**, 1028 (1994).
[28] A. B. Rechester and M. N. Rosenbluth, Phys. Rev. Lett. **40**, 38 (1978).
[29] S. Ortolani (private communication, 1998).
[30] V. Antoni, D. Merlin, S. Ortolani, and R. Paccagnella, Nucl. Fusion **26**, 1711 (1986).
[31] J. B. Taylor, Rev. Mod. Phys. **58**, 741 (1986).
[32] Z. X. Jiang, A. Bondeson, and R. Paccagnella, Phys. Plasmas **2**, 442 (1995).
[33] W. A. Newcomb, Ann. Phys. (N.Y.) **10**, 232 (1960).
[34] H. P. Furth, J. Killeen, and M. N. Rosenbluth, Phys. Fluids **6**, 459 (1963).
[35] J. P. Freidberg, Rev. Mod. Phys. **54**, 801 (1982).